Available online at www.sciencedirect.com
SCIENCE DIRECT®
Progress in Oceanography 63 (2004) 57–98
Progress in Oceanography
www.elsevier.com/locate/pocean

A multi-year record of hydrographic and bio-optical properties in the Gulf of Maine: I. Spatial and temporal variability

W.M. Balch [a,*], D.T. Drapeau [a], B.C. Bowler [a], E.S. Booth [a], J.I. Goes [a], A. Ashe [b], J.M. Frye [c]

[a] *Bigelow Laboratory for Ocean Sciences, P.O. Box 475, McKown Point Road, West Boothbay Harbor, Maine, ME 04575, USA*
[b] *College of Ocean and Atmospheric Sciences, Oregon State University, 104 Ocean Admin Building, Corvallis, Oregon 97331-5503*
[c] *Scotia Prince Cruises, P.O. Box 4216, Portland, ME 04101-0416*

Received 30 August 2002; revised 26 August 2004; accepted 13 September 2004

Abstract

A three year time series of hydrographic and optical data was acquired in the Gulf of Maine using a passenger ferry as a sampling platform; the ferry sails regularly between Yarmouth, Nova Scotia, Canada, and Portland, Maine, USA. The sampling program was designed to provide a time series of spatial information on temperature, salinity, phytoplankton abundance, and inherent optical properties (IOPs) of surface waters. Significant interannual differences were observed in the hydrography. The average vertical temperature gradient over the upper 50 m (measured with XBT's) was inversely correlated with density at 2 m depth, demonstrating a strong connection between the surface water properties sampled from the ferry and those of the euphotic zone. Highest chlorophyll *a* concentrations were recorded at hydrographic boundaries, particularly at a frequently-observed offshore extension of the Eastern Maine Coastal Current, south of Penobscot Bay, ME. XBT results showed the intrusion of Maine Bottom Water on time scales of 20–45 d that occurred during late spring or early summer. The optical scattering (at 412 nm) of particulate and dissolved material was highest in the Western Maine Coastal Current (WMCC), but high values were also observed in Scotian Shelf Water (SSW). Typically, spatial patterns of backscattering mirrored total scattering. Acid-labile backscattering (representative of suspended calcium carbonate) was usually 20% of the total particulate backscattering. It reached as high as 80% of the total backscattering during a coccolithophore bloom in 2000, which occurred at the hydrographic boundary between SSW and Jordan Basin Water. Backscattering probability (backscattering/scattering) was usually <1% and showed gradual changes over the season, with lowest values in the late summer/early fall. The shape of the volume scattering function (VSF; defined as the scattered intensity per unit incident irradiance per unit volume) for particulate material was significantly different than that reported by Petzold (1972), and this difference showed coherent variability over time and space. The average chlorophyll *a* concentration measured over the entire Gulf was positively correlated with the volume of Maine Surface Water present. Dissolved and detrital material was weakly colored and most abundant

* Corresponding author. Tel.: +207 633 9600; fax: +207 633 9641.
E-mail address: bbalch@bigelow.org (W.M. Balch).

0079-6611/$ - see front matter
doi:10.1016/j.pocean.2004.09.003

in the WMCC, and it contained components with significant absorption *and* scattering. We report a minimal abundance of Case I surface water (i.e., water with inherent optical properties indexed to phytoplankton and their associated constituents) in the Gulf of Maine. The majority of the surface water was Case II for particles, as well as Case II for dissolved and detrital material (where "Case II" indicates water with inherent optical properties dominated by materials other than phytoplankton, such as suspended sediments or colored dissolved organic matter from rivers). Particle-laden Case II water in the Gulf of Maine had a weak but significant correlation with CDOM and detritus-dominated Case II water. The sources of these Case II waters appear to be both inside and outside the Gulf of Maine.

Keywords: Gulf of Maine; Backscattering; Absorption; Volume scattering; Colored dissolved organic matter; Calcium carbonate; Optical Case II waters; 42°N; 68°W

1. Introduction

Our understanding of ocean biogeochemistry on long time scales relies on multidisciplinary observations from a variety of platforms. Time series measurements have provided the opportunity to document the biological response to large-scale forcing over annual and decadal time scales. A few of the more notable time series stations are: Ocean Station S in the North Atlantic Ocean (Joyce & Robbins, 1996; Schroeder & Stommel, 1969), Ocean Station Papa in the North Pacific Ocean (Wong et al., 1999), Ocean Station Bravo in the Labrador Sea (Sathiyamoorthy & Moore, 2002), the Southern California Bight Study (Eppley, 1986), NOAA Coastal Ocean Time Series and the MARMAP study in the Northwest Atlantic Continental Shelf waters (Campbell & O'Reilly, 1988), CalCoFI (Reid, 1988), Hawaiian Ocean Time Series and Bermuda Atlantic Time Series (Siegel, Karl, & Michaels, 2001), and the European Station for Time-Series in the Ocean Canary Island (Davenport et al., 1999).

Advection of coherent mesoscale features past a single sampling point can obscure the true temporal variability representative of an entire region. Optimal time series sampling strategies, therefore, should include both temporal and spatial sampling, but this is often cost-prohibitive. Two of the better examples of a time series documenting both spatial and temporal variability are CalCOFI (Reid, 1988) and the Atlantic Meridional Transect work, which spans entire ocean biomes between 50°S and 50°N (Aiken et al., 2000).

There are strong horizontal gradients in physical and biological variables within shelf regions due to stronger advection and enhanced vertical mixing. Deconvolving spatial versus temporal variability of physics and biology, therefore, is difficult in the coastal zone unless a multiple station design is used. This is well demonstrated in satellite images of temperature or chlorophyll pigments in which the spatial variability of physics and algal biomass near the coast are highly dynamic and well correlated. Yentsch and Garfield (1981) reported one of the first satellite observations for the Gulf of Maine, showing gradients in temperature and chlorophyll pigments orders of magnitude greater than in the central oceans.

Not until the last decade have optical measurements become a regular part of time series studies (e.g., HOTS and BATS, Dickey et al., 2001; CalCOFI and Monterey Bay time series, Chavez, Herlien, & Thurmond, 1994; Kuo, 1991). This situation is improving with the advent of localized ocean observing systems such as LEO-15 (Grassle, Petrecca, & von Alt, 1995) and global ocean observing systems (e.g., the Gulf of Maine Ocean Observing System, implemented in 2001, Bogden, 2002; Pettigrew et al., 2002), as well as time series of satellite measurements (e.g., AVHRR, SeaWiFS, MODIS) that provide both temporal and spatial information relevant to the variability of phytoplankton populations. Moreover, optical time series, particularly in coastal settings, provide valuable information about phytoplankton abundance, plus concentrations of detritus and colored dissolved organic matter. This last component contributes a variable fraction of the total ocean dissolved organic carbon pool, the largest single organic carbon pool in the sea (Hansell & Carlson, 2001). Thus, inclusion of ship-board optical measurements as part of time series studies is critical for understanding the environmental controls on these carbon pools.

1.1. The Gulf of Maine: A geostrophic estuary

The Gulf of Maine is a continental shelf sea off the NE coast of the US with a maximum water depth of ~275 m. It has a temperate/boreal climate and supports high primary production and various large fisheries. Probably the single most important factor affecting the biological production (and optics) of the Gulf of Maine is the intrusion of deep slope water with salinity >34 (originally described by Bigelow (1927)) through the Northeast Channel, which overflows into the Jordan, Wilkinson, and Georges Basins (Townsend, 1989, 1991) (Fig. 1). The intrusions overflow a 230 m sill and are thought to consist of both warm slope water and Labrador slope water, with average transport of $\sim 262\ (\pm 58) \times 10^3\ m^3\ s^{-1}$ occurring in strong pulses lasting 4–11 d and driven by wind stress-induced, barotropic, pressure gradients (Ramp, Schlitz, & Wright, 1985). Such intrusion events are a source of dissolved inorganic nitrogen, and they provide new nitrogen to the entire region, supporting biological production when mixed into well-illuminated surface waters. Nutrient ratios in the Gulf of Maine could be influenced by the North Atlantic Oscillation (NAO), in that positive and negative NAO indices are associated, respectively, with (a) warm southern slope water or (b) cold Labrador slope water propagating into the Gulf (Drinkwater, Mountain, & Herman, 1999). These two water types appear to have different N:Si ratios (D. Townsend, per. comm.) leading to the intriguing hypothesis that the relative distributions and concentrations of diatoms and non-silicified phytoplankton could vary interannually in response to the NAO.

Upward mixing of deep water is thought to occur during strong convective overturn events in winter (Brooks, 1992), which can result in the formation of Maine Intermediate Water (MIW) from the admixture of low salinity surface water and the deeper Maine Bottom Water (Hopkins & Garfield, 1979) (note, the cooling of Maine Surface Water can also contribute to MIW formation, Brooks, 1985). Inflow of fresh water during spring runoff, contrasting with dense slope water intrusions in the basins, induces a topographic low in the middle of the Jordan Basin of the Gulf of Maine and a geostrophic counterclockwise (CCW) surface circulation. This CCW flow was originally inferred by Bigelow (1927). The intensity of this gyre as well as Gulf of Maine-wide nitrogen input, are related to the volume of deep water advected into the

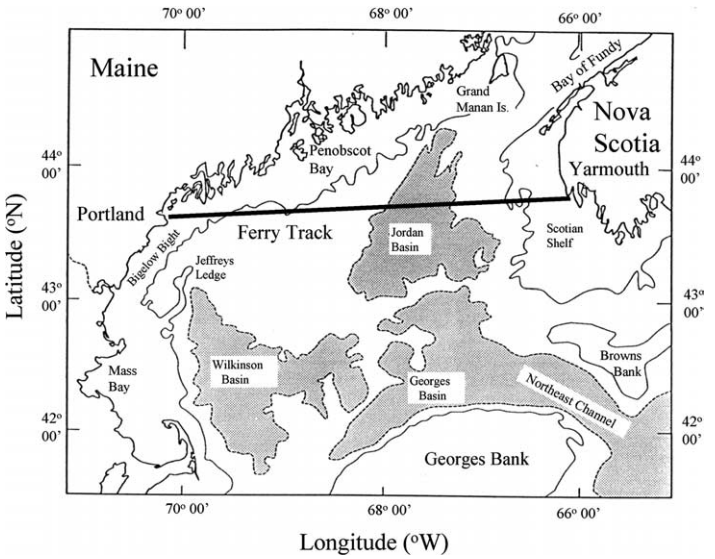

Fig. 1. Map showing banks, bays and basins of the Gulf of Maine (modified from Figure 1 of Townsend (1991)). Ferry track shown as a heavy black line. Fine black lines designate the 100 m isobath and dashed lines designate the 200 m isobath.

basins, which is inversely related to freshwater runoff (Brooks, 1992; Brooks & Townsend, 1989; Townsend, 1991). Most of the variance in the CCW Maine Coastal Current circulation (affecting its nutrient chemistry and biology) is associated with time scales exceeding 1–2 months; this variability appears to be driven by low frequency changes in the Jordan Basin Water (JBW) (Bisagni, Gifford, & Ruhsam, 1996).

Terminology varies for the various aspects of the CCW flow around the JBW, but there are some commonalities (Brooks, 1985; Lynch, Holboke, & Naimie, 1997; Pettigrew et al., 1998). On the eastern side, cold, fresh Scotian Shelf Water (SSW) enters the Gulf of Maine along the southern coast of Nova Scotia, south of Cape Sable (Smith, 1983, 1989). The SSW can be influenced by lower salinity water flowing from the Gulf of St. Lawrence, taking about 9 months until it enters the Gulf of Maine (Sutcliffe, Loucks, & Drinkwater, 1976). SSW proceeds into the Bay of Fundy where it is mixed by intense tides (Bisagni et al., 1996) (which also resuspend significant amounts of sediment). On the western side of the Gulf of Maine, the CCW circulation consists of the cold Eastern Maine Coastal Current (EMCC), which generally flows westward along isobaths parallel to the coast. Cold surface temperatures of the EMCC are indicative of its SSW source. The EMCC flow branches off Penobscot Bay, the portion going offshore is known as the "offshore extension of the EMCC" (Bisagni et al., 1996; Pettigrew et al., 1998). This offshore extension can be observed in AVHRR imagery of SST between April to November (it is harder to see in the winter months when there is barely any temperature contrast between the coastal waters and central gulf). The plume appears to be a significant source of nitrate to JBW (Pettigrew et al., 1998). From Penobscot Bay to Cape Cod, the coastal current is called the Western Maine Coastal Current (WMCC; Brooks, 1985). While still debated, the EMCC may partially feed into the WMCC. Western Maine coastal waters are warmer than the EMCC and less saline due to added river input.

Townsend (1998) suggested, using a box model, that the deep water influxes of new nitrogen were insufficient to drive the observed new production of the Gulf of Maine (see also Ramp et al. (1985)). Instead, he suggested that nitrification rates are high enough (Christensen, Townsend, & Montoya, 1995) that the nitrate derived from the primary nitrite maximum (Holligan, Balch, & Yentsch, 1984) (associated with Maine Intermediate Water) could be mixed into surface waters during convective overturn events or along frontal boundaries (Yentsch & Garfield, 1981) and support a significant fraction of new primary production. An important caveat to this interpretation is that, for lack of data, Townsend assumed that imports and exports of dissolved organic nitrogen were equal. Given the significant freshwater runoff, there potentially could be large pools of terrestrially-derived DON which could act as an allocthonous source of nitrogen for bacteria, which, through decomposition and subsequent nitrification, could potentially fuel new production. While nitrification within the Gulf of Maine most definitely supports new nitrate production, the largest source of nitrate will likely have come through the NE Channel as North Atlantic Slope Water, at the surface as SSW, or out of rivers. Sampling strategies that follow the relative importance of each water mass over time will provide the most insight into factors regulating primary production of the region.

Long-term hydrographic variability and its influence on ocean productivity are not well understood in the Gulf of Maine, which is quite remarkable, especially considering that the Gulf of Maine has been intensively studied beginning with the work of Bigelow (1914, 1926). The largest sampling program was the MARMAP program, but primary production measurements were not made on a uniform station grid, which made comparisons between cruises and over time difficult. The advent of ocean color remote sensing demonstrated highest chlorophyll levels in the Eastern Maine Coastal Current (Yentsch & Garfield, 1981), suggestive of higher primary production in this region. Even this information was hard to interpret, however, as little was known about the Gulf's optical properties and how much of the Gulf water was Case I (i.e., water with inherent optical properties dominated by phytoplankton and their associated materials) versus Case II (i.e., waters with inherent optical properties dominated by constituents other than phytoplankton, such as sediments or colored dissolved organic matter). Given the periodic, significant riverine run-off and sediment resuspension associated with intense tidal mixing, large amounts of Case II waters could compromise the accuracy of ocean-color algorithms (O'Reilly et al., 1998), giving false high chloro-

phyll values. Frequent blooms of the coccolithophore, *Emiliania huxleyi*, also could compromise ocean-color pigment algorithms, causing underestimates in pigment concentrations (Balch, Eppley, Abbott, & Reid, 1989). Thus, one of the major hurdles in understanding phytoplankton primary production in the Gulf of Maine is the development of general satellite algorithms for interpreting ocean color measurements (Campbell & O'Reilly, 1988). The fundamental problem is that there are limited simultaneous ship and satellite data to (a) quantify the inherent optical properties (IOPs) and apparent optical properties (AOPs) necessary for algorithm development (Fargion & McClain, 2000), and (b) to decide which optical algorithms to use, Case I or Case II (Gordon & Morel, 1983).

This is the first paper of a series describing a field program in which a passenger ferry in the Gulf of Maine was used as a platform to collect sea-truth hydrographic and bio-optical data. The idea came from a ferry-based project in 1982 along the same cruise track for examining chlorophyll, hydrography and zooplankton (Bisagni et al., 1996; Boyd, 1985). In this earlier work, the ferry provided an inexpensive, convenient sampling platform with a consistent cruise track across the Gulf. In the work described herein, the flexibility of this ferry-based approach also allowed us to plan cruises for clear-sky days when satellite coverage was optimal (which also provided significant savings in ship costs since we could be selective about which days we sailed). The satellite data will be discussed in a separate communication. The results to be presented here are the basis for a Gulf of Maine time series with the primary goal of elucidating the seasonal and interannual relationships between hydrography, ocean color and algal biomass in the Gulf of Maine. While measurements are still ongoing, we report our findings from the first 3 years of this time series and discuss the relationships between hydrography and bio-optics of the Gulf of Maine.

2. Methods

2.1. Ship sampling

All data collected in this study were taken aboard the *M/S Scotia Prince* (Scotia Prince Cruises, Portland, ME), a 144 m long car/passenger ferry that travels between Yarmouth, Nova Scotia, Canada, and Portland, Maine, USA, maintaining a speed of 18–20 kts. (9.3–10.3 m s^{-1}) in sea states up to Force 7. We converted a standard shipping container into a small laboratory and carried it aboard the ferry on the back of a flatbed truck. The ship operated between 15 May and 31 October, departing Portland, ME each day at 21:00 h EDT, and arriving 11 h later in Yarmouth, NS at 08:00 EDT the next morning. Following a 1 h layover in Yarmouth, the ship departed at 09:00 h EDT, and returned to Portland by 20:00 h EDT, with another 1 h layover before its next trip. Results to be presented here were collected during daylight trips from Yarmouth to Portland, only on clear-sky days for maximum coverage by ocean color satellites (Table 1). The cruise track from Yarmouth, NS passed Cape Fourchu (Yarmouth entrance) and German Bank, then across Jordan Basin on a course of 267° (true bearing), then just north of Jeffreys Bank, toward Witch Rock, and finally Portland Harbor (Fig. 1). During 1998 and 1999, surface seawater was sampled from 1 to 2 m below the surface using an exterior-mounted, stainless-steel sampling pipe. In 2000, a non-toxic, stainless steel sample line was installed off the ship's sea chest which supplied water from ~2.5 m depth, to our portable laboratory container, parked 30 m aft of the sampling locations on the ship. Water flow to the instrumentation was started ~1/4–1/2 h after departure from Yarmouth, and data collection began at the Cape Fourchu marker. The length of the entire transect was ~330 km, and data typically were collected for 290–330 km of the trip. For statistical analyses involving comparisons of multiple cruises, data were standardized geographically to include locations between Cape Fourchu and 69.6°W. West of this longitude (or typically about 1.5 h prior to arrival in Portland), our sampling systems were turned off and stowed for disembarkation. Note, on several occasions, trips were run on consecutive days.

Table 1
Summary of Gulf of Maine data taken from *M/S Scotia Prince* from 1998 to 2000

Activity	1998	99	2000	Total
No. cruises	10	20	12	42
No. ac-9	1388	2917	2012	6317
No. b_b (Wyatt)	1460	3290	2012	6762
No. b_b (HS-II)	0	3290	2012	5302
No. Temp/Sal	1460	3290	2012	6762
No. XBT profiles (1 per h)	85	171	96	352
No. chlorophyll	1421	3290	2012	6723

Each measurement of optical properties, hydrography, or chlorophyll *a* represents an average over ~2.2 km of horizontal distance.

In this case, we did not have to disembark from the ship after the first day and this allowed seawater sampling all the way to Portland.

2.2. Flow-through system

The flow-through system in our portable lab container made a suite of hydrographic and inherent optical property (IOP) measurements. Data integration and logging were done by National Instruments LabVIEW software, run on two Pentium processor computers. The system received time and logged the ship's geographic position continually from a Garmin 220 global positioning system, with the antenna mounted outside the ship, within 10 m of the laboratory van. For all measurements, any changes in instrument calibration were applied linearly between consecutive calibrations (see specific calibration details for the various instruments described below).

Seawater first entered a vortex de-bubbler (SUNY VDB1), then flowed into a second 1.2 m tall, linear de-bubbler, equipped with a 1 mm screen to keep the largest zooplankton and salps out of the optical instruments (which improved data quality significantly). Next, the flow entered an InterOcean TempSal thermal conductivity sensor. It measured salinity with an accuracy of ±0.05 PSS (Practical Salinity Scale) and temperature to an accuracy of ±0.1 °C.

The remainder of the flow-through measurements were meant to describe the fundamental optical properties of the suspended particles and colored dissolved constituents, for relation to the hydrographic results. From the thermosalinograph, flow entered into a Turner 10AU-005-CE fluorometer for monitoring underway chlorophyll *a* fluorescence. The fluorometer was equipped with a daylight white F4T5D lamp, blue-violet excitation filter (peak excitation 438 nm with half bandpass of 340–500 nm) and red emission filter (high pass >665 nm interference filter). To insure against bio-fouling, the fluorometer was cleaned regularly. Underway fluorescence measurements were calibrated to chlorophyll *a* concentration using hourly discrete samples (in triplicate).

Water then flowed into a tertiary debubbler and was sampled via a diaphragm metering pump, into a Wyatt Technologies Model "Dawn F" laser light scattering photometer for measurements of volume scattering (defined as the scattered intensity per unit incident irradiance per unit volume). The description of volume scattering as a function of angle is known as the volume scattering function (VSF). The flow rate through the Wyatt instrument was ~11–15 ml min^{-1}. The photometer operated with a 10 mW Argon ion laser (514 nm) which was directed into the center of a flow-through cuvette, whereupon, volume scattering was measured by 15 photodiodes arranged between 21.54° and 158.14° around the incoming laser beam. Two additional photodiodes were utilized for laser power monitoring (one in front of the viewing cuvette, and one after the cuvette). The laser beam had a $1/e^2$ gaussian beam profile radius of 0.39 mm which made the effective viewing volume of the light-scattering photometer ~0.25 μl. All detectors were scanned at rates of 200 Hz which insured that the same sea water volume was not sampled twice.

Total backscattering was estimated by the Dawn F light scattering photometer by fitting a line to the volume scattering measurements (to derive the VSF), then integrating the VSF in the backwards direction (Balch, Drapeau, Fritz, Bowler, & Nolan, 2001; Balch et al., 1999). Backscattering of particulate plus dissolved material ($b_{b\ pg}$) was calculated by subtracting pure water backscattering coefficients (Mobley, 1992) from the total backscattering. The backscattering measurement and data analysis are described in more detail elsewhere (Balch & Drapeau, 2004, Chapter 4). Backscattering data and associated statistics were typically logged every ~50 s (which represented an effective volume sampled of 9–12.5 ml).

To understand scattering variability in the sea, it is important to address the underlying VSF. To this end, we compared the shape of the average VSF from the Gulf of Maine to Petzold's classic data (Petzold, 1972), derived from San Pedro Channel, California. In order to focus on the shape of the VSF, Gulf of Maine volume scattering data at each angle (θ) were normalized to the 90° volume scattering value ($\beta_{\mathrm{norm}^{\theta}}$). Petzold's coastal volume scattering data similarly were normalized to the 90° volume scattering (using Table 3.10 of Mobley (1994)), then interpolated to the same angles as our Wyatt Technologies instrument ($\beta_{\mathrm{normPetzoldInterp}^{\theta}}$). The % difference of our normalized data from the interpolated, normalized Petzold coastal water was calculated as: $\%\ \mathrm{difference} = [(\beta_{\mathrm{norm}^{\theta}} - \beta_{\mathrm{normPetzoldInterp}^{\theta}})/\beta_{\mathrm{normPetzoldInterp}^{\theta}}] \times 100$. The importance of this equation is that it allows one to describe, for a given scattering angle, how the volume scattering differs from the classic shape of the volume scattering function commonly assumed in hydrological optics.

Because of our interest in suspended calcite (otherwise known as particulate inorganic carbon or PIC) from coccolithophores, we also measured volume scattering before and after dissolution of any suspended $CaCO_3$. Following the first 50 s of measurements on raw sea water, a peristaltic pump was activated by the LabVIEW control system, which injected 0.5% glacial acetic acid into the flow stream and dispersed it using a Teflon mixing coil. This dropped the measured pH to ~5.8 to dissolve $CaCO_3$ (Berner, 1976). Once the pH stabilized at the more acidic value, volume scattering was re-sampled for 20–50 s and average backscattering re-calculated. The difference between the raw and acidified backscattering values represented the "acid-labile" backscattering (b'_b). Using field measurements, we calibrated this acid-labile backscattering to atomic absorption estimates of suspended calcite concentration and performed an error analysis (see Balch et al. (2001)). The acidification cycle was adjusted to run one complete raw/acidification cycle approximately every 4 min. This means that the semi-continuous ship data were averaged over ~2.2 km. Absolute calibration of the light scattering photometer was based on the known scattering properties of methanol or toluene (analytical-grade, 0.02 μm-filtered). Pre- and post-cruise calibrations of the light-scattering photometer were performed with ultra pure, 0.02 μm-filtered, distilled water; this allowed a bio-fouling correction to be applied to the data. Any observed change in instrument calibration due to biofouling was linearly interpolated and applied to each datum. Due to the fact that acid was being added periodically to the seawater flowing through the Wyatt instrument, this water was discarded following measurement. Based on flow-through measurements using "particle-free" water (filtered through a 0.02-μm pore size filter), measurements of volume scattering at 90° were good to within $\sim\pm 1.5 \times 10^{-4}\ \mathrm{m}^{-1}\ \mathrm{sr}^{-1}$. This error included calibration error and bio-fouling effects on the flow-through cuvette during continuous use.

Water exiting the fluorometer flowed into an "ac-9" (WET Labs, Philomath, Oregon), which continually measured optical absorbance and attenuation of seawater at nine wavelengths using a dual-path optical scheme.Temperature and salinity data taken with the InterOcean TempSal thermal conductivity sensor were used in the temperature-salinity correction required by the WET Labs ac-9 protocol (Pegau, Gray, & Zaneveld, 1997). To correct absorption measurements for scattering errors, we used method 3 from the WET Labs ac-9 protocol (http://www.wetlabs.com/Products/pub/ac9/ac9proti.pdf). This correction assumes that there is a reference wavelength for which the absorption coefficient of dissolved plus particulate materials is zero. It also assumes that the shape of the VSF is independent of wavelength. The correction scheme essentially requires two attenuation values, two absorption values, temperature, salinity and calibration water temperature and salinity. The ac-9 was sent to the manufacturer for calibration annually.

The factory-stated accuracy of the attenuation and absorption measurements was $\pm 0.005\ m^{-1}$ with linearity error of ±0.1%. A dry calibration and a wet calibration (using 0.2 μm-filtered, MilliQ water) were performed before each 11 h transect according to standard protocols supplied with the instrument. A wet calibration was performed at the end of each trip, as well. Any change in calibration due to biofouling was corrected by linearly interpolating the change over time between the pre- and post-cruise wet calibration. During regular sampling operations, attenuation and absorption values for particle-free sea water (Smith & Baker, 1981) were subtracted in order to derive total particulate and dissolved attenuation (c_{pg}) and absorption (a_{pg}). These data were then used to derive the total scattering of particulate and dissolved material, b_{pg} ($=c_{pg} - a_{pg}$). For the 2000 field season, an in-line solenoid valve system was added upstream of the ac-9, which directed flow through a filtration manifold about every 2 min thus removing particulate matter >0.2 μm. Once the ac-9 equilibrated with the filtered water (~1 min.) data were logged, after which flow reverted back to unfiltered seawater. Over each 4 min segment of the voyage, the ac-9 measurements of a and c were made of total particulate plus dissolved matter, as well as for water/particles passing a 0.2 μm filter (hereafter referred to as colored dissolved organic matter, or CDOM). The difference between the total and filtered ac-9 measurements provided a and c values of the particles >0.2 μm only. This sampling design (one ac-9 with alternating unfiltered and >0.2 μm filtered flow) allowed elimination of errors involved in intercalibrating two ac-9s.

For the 1999 and 2000 field seasons, flow-through surface water also was viewed by a HOBI Labs Hydroscat-2. This instrument was set to view an enclosed, 21-liter, sand-blasted, stainless steel container (painted flat black within). The instrument measured volume scattering at 142°, which was extrapolated to the backscattering coefficient using an assumed VSF (Maffione & Dana, 1997). It estimated backscattering at two wavelengths (470 and 676 nm) plus chlorophyll fluorescence at 676 nm. The two estimates of backscattering were then used to estimate the wavelength dependence of backscattering between 470 and 676 nm. The light sources in this instrument pulsed at different times so that the backscattering at the two wavelengths could be differentiated from chlorophyll fluorescence induced by the 470 nm light source. That is, the backscattering measurements were made using the synchronous 470 nm incident source and 470 nm detection or 676 nm incident source and 676 nm detection, respectively. The HOBI Labs fluorescence measurement used the gated 470 nm excitation combined with the 676 nm detector. It was calibrated at the factory annually. The combined scattering and absorption properties measured in this study, together with the hydrological measurements, allowed us to examine whether water masses of the Gulf of Maine could be discriminated according to not only temperature and salinity, but also their inherent optical properties.

2.3. Depth profiles of temperature

Hourly XBT profiles were used to construct a temperature vs. depth section between Yarmouth and Portland for each trip. Data were binned to 1 m averages. Upon completion of each trip, data were contoured using Surfer© software and the mixed layer depth was estimated based on the depth at which the temperature changed 0.1 °C from the surface value. Note, the temperature data from the XBT probes typically were not used in the top 1 m due to probe equilibration after the warm probe contacted the cold seawater. After contouring of the data, the matrix of depth, horizontal distance and temperature (with spatial resolution of 1 m vertically and ~3 km horizontally) was examined for water mass qualities. The area of each section containing water of a given temperature range was calculated and converted to the fraction of the total cross-sectional area that contained a specific water mass. While defining a water mass based on temperature alone (without salinity) obviously is not possible with only XBT data, this temperature-based analysis allowed crude interannual comparisons to be made concerning the relative importance of the various water masses. Due to the frequent presence of temperature inversions in the deep Gulf of Maine from North Atlantic slope water intrusions (Brooks, 1985; Mountain & Jessen, 1987), separate calculations were made for deep and shallow pools.

Consistent with Brooks (1985), Maine Bottom Water (MBW) was defined as water deeper than the surface mixed layer (uppermost 50 m) with temperatures exceeding 7 °C. Maine Surface Water (MSW) was defined as water above 50 m with temperatures exceeding 7 °C (note, the coldest surface water observed was never colder than 8 °C). Maine Intermediate Water (MIW) (Hopkins & Garfield, 1979) was defined as water below the surface mixed layer with temperatures <7 °C.

2.4. Discrete samples

Every hour, a surface water sample was taken to measure extracted chlorophyll *a* for use in calibrating the continuous fluorescence measurements. Aliquots were also filtered for particulate organic carbon and nitrogen (POC and PON, respectively) plus PIC. Chlorophyll *a* and POC/PON samples were filtered through Millipore H/A© and baked Gelman GF/F© filters, respectively, and measured according to the JGOFS protocols (JGOFS, 1996). PIC samples were filtered through 25 mm diameter, 0.4 μm poresize, polycarbonate filters, and measured according to Balch, Drapeau, and Fritz (2000) except that an inductively-coupled plasma atomic absorption spectrometer was used to measure calcium instead of a graphite furnace atomic absorption spectrometer. A complete list of the discrete variables sampled and their respective units is given in Fargion and McClain (2001).

3. Results

3.1. Data set limitations

Before pointing out the notable features of this large data set, it is important to point out a few of its limitations. The ferry operated between May and October of each year, but during the first year of the program (1998) data collection was confined to September and October only, whereas in 1999 and 2000 cruises were performed throughout the entire ferry season. Moreover, due to the timing of the cruises to clear-sky events with good satellite overpasses, sampling intervals for this work were not constant. This means that ship measurements have weather biases (mostly clear skies with winds out of the NW). A summary of the data collected during the first three years of ferry sampling is given in Table 1.

3.2. Spatial and temporal variability in hydrography and chlorophyll

With the above caveats in mind, there were several aspects of the hydrography worth noting. Due to the large volume of data collected in this study and large number of figures necessary to describe it, the raw data plotted as a function of longitude have been archived on the world-wide web as Multi-Media Components (doi:10.1016/j.pocean.2004.09.003), and these figures will be cited with MMC before the figure reference (e.g., MMC Fig. 1). These figures will not appear in this paper. All references to figures that appear in this manuscript will be made without the MMC prefix. In the event the reader does not have access to the worldwide web, we present results from selected cruises within this paper. These cruises were made during approximately the same time each year: early June (day 157, 1999 and day 156, 2000; Fig. 2), late June (day 172, 1999 and day 176, 2000; Fig. 3), late August (day 235, 1999 and 2000; Fig. 4), and early October (day 277, 1998; day 281, 1999; day 274, 2000; Fig. 5). Note, the cruise track was almost east-west, allowing the data to be plotted against longitude. To convert longitude in any of the figures in this paper (where negative longitude signifies degrees west) to distance from the Yarmouth channel marker (in kilometers), use the following relationship, derived empirically from our data: $\text{Distance} = -80.4705 * \text{Longitude} - 5323.68$.

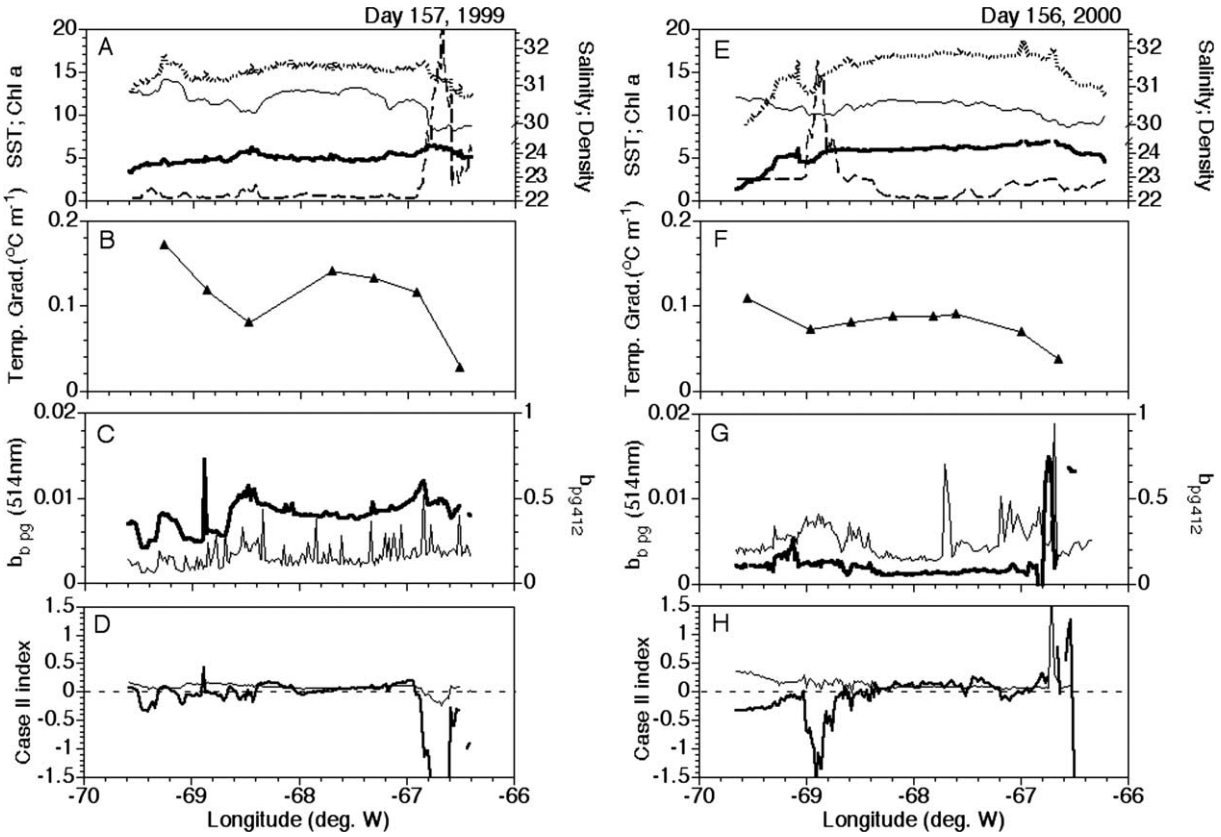

Fig. 2. Examples of Gulf of Maine data from day 157, 1999 and day 156, 2000, all plotted against longitude. Panels A and E sea surface temperature (SST; °C; fine black line), chlorophyll a (μg Chl *a* L^{-1}; dashed line), salinity (hatched line) and density (sigma theta units; heavy black line); Panels B and F temperature gradient from 1 to 50 m; Panels C and G Total particulate and dissolved backscattering at 514 nm (m^{-1}; fine solid line) and 412 nm scattering (heavy solid line), Panels D and H Case II_{partic} index (heavy solid line) and Case II_{diss} index (fine solid line).

3.3. Sea surface temperature

Generally, the range of sea surface temperature (SST) along the complete transect was greatest in mid-summer (8 °C) and decreased in spring and fall (to as little as 1.5 °C; Figs. 2–5). Highest temperatures were observed during days 260–261 of 1998 (MMC Fig. 1, lines A and B; but recall that we only began sampling in September of that year), between days 214 and 257 during 1999 (MMC Fig. 2, lines G–M) and days 235 and 258 during 2000 (MMC Fig. 3, lines I–K). The pattern of SST across the Gulf showed consistently coolest temperatures in the SSW with increasing temperatures associated with JBW. There was a consistent decrease in temperature associated with the offshore extension of the EMCC and a warming associated with the WMCC (Panels A and E, Figs. 2–4; MMC Figs. 1, 2, 3). Temperature peaks were associated with the WMCC or JBW, often both. Despite the reduced number of months sampled in 1998, SST was ~2 °C colder than 1999 or 2000 during the same time period (after day 260; compare SST traces in Fig. 5A, E, and I). The temperature gradients in the upper 50 m were also greater in fall of 1998 (see Fig. 5B, F and J). Fall mixing significantly reduced the surface temperature variability across the entire Gulf to <3 °C by day 293 of 1998, day 267 of 1999, and day 274 of 2000 (MMC Fig. 1 line J, MMC Fig. 2 lines N–R, and MMC Fig. 3 line L).

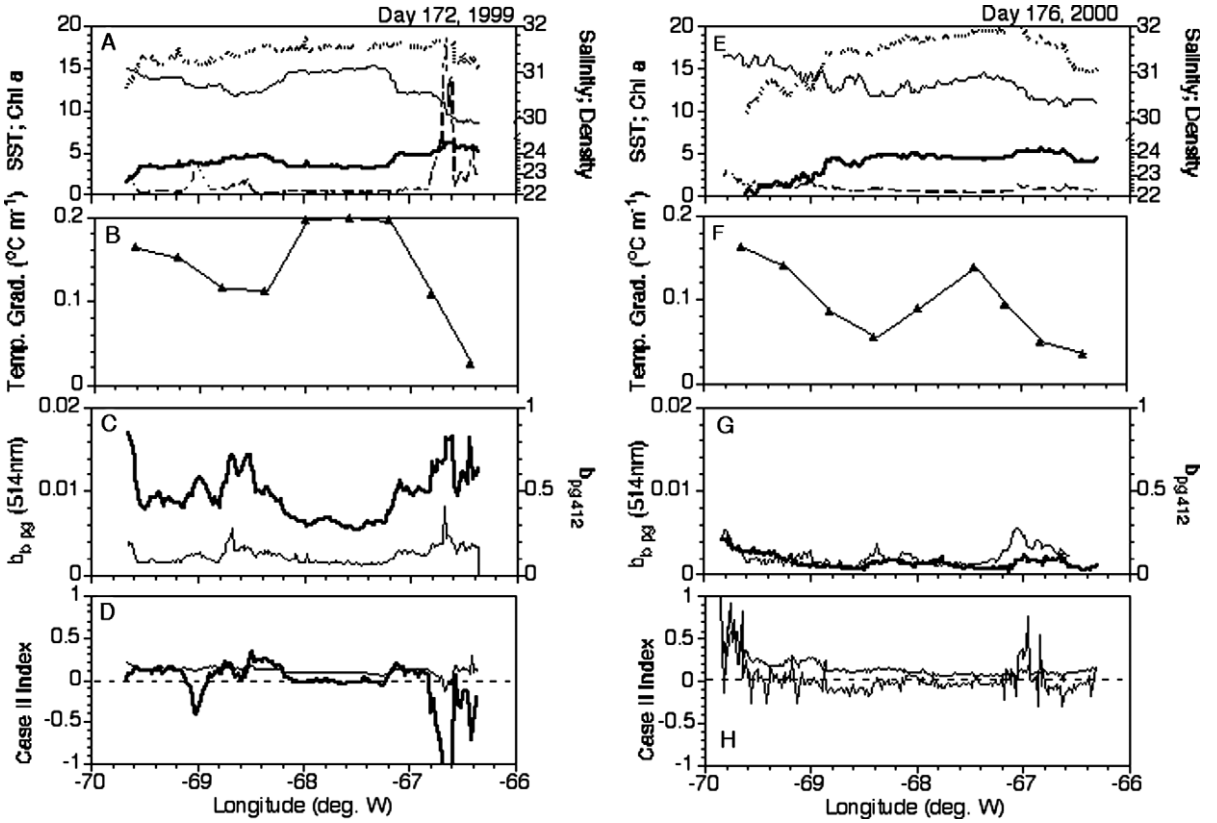

Fig. 3. Examples of Gulf of Maine data from early summer for day 172, 1999 (panels A–D) and day 176, 2000 (panels E–H), all plotted against longitude: Key to different lines same as in Fig. 2.

3.4. Salinity

Highest salinities (~33 PSS) were almost always observed in the JBW. Fresher (and usually warmer) water was observed in the WMCC, while fresher (and cooler) water was seen in the Scotian Shelf region (Figs. 2–5; MMC Figs. 4, 5, 6). On average, salinities increased through the sample period (~1PSS over 160d). The ship often passed through a low salinity plume between ~69°W and 69.5°W longitude, the offshore extension of the EMCC (Figs. 2A and E, 3A, 4A and E, 5E; MMC Fig. 4 line D, MMC Fig. 5 lines B,C, F, G, H, O, P, Q, R; MMC Fig. 6 lines A–H, K). When trips were run on consecutive days, we could sample seawater all the way to Portland on the first day (since we did not need to disembark from the ferry). On these occasions, the lowest salinity WMCC water was observed near Portland Harbor (MMC Fig. 4 lines A, F, H; MMC Fig. 5 lines A, D, E, K, L, N; MMC Fig. 6 lines C, G).

3.5. Density

The broad pattern of density showed highest values in SSW, and lowest values in the fresh waters of the WMCC (Figs. 2–5; MMC Figs. 7, 8, 9). Superimposed on this pattern was a seasonal density decrease in the Jordan Basin, associated with surface heating (e.g., Figs. 2A, 4A; MMC Fig. 7 lines A–D; MMC Fig. 8 lines A–L; MMC Fig. 9 lines E–K). During late summer (e.g., day 255, 256 of 1999), there was considerable

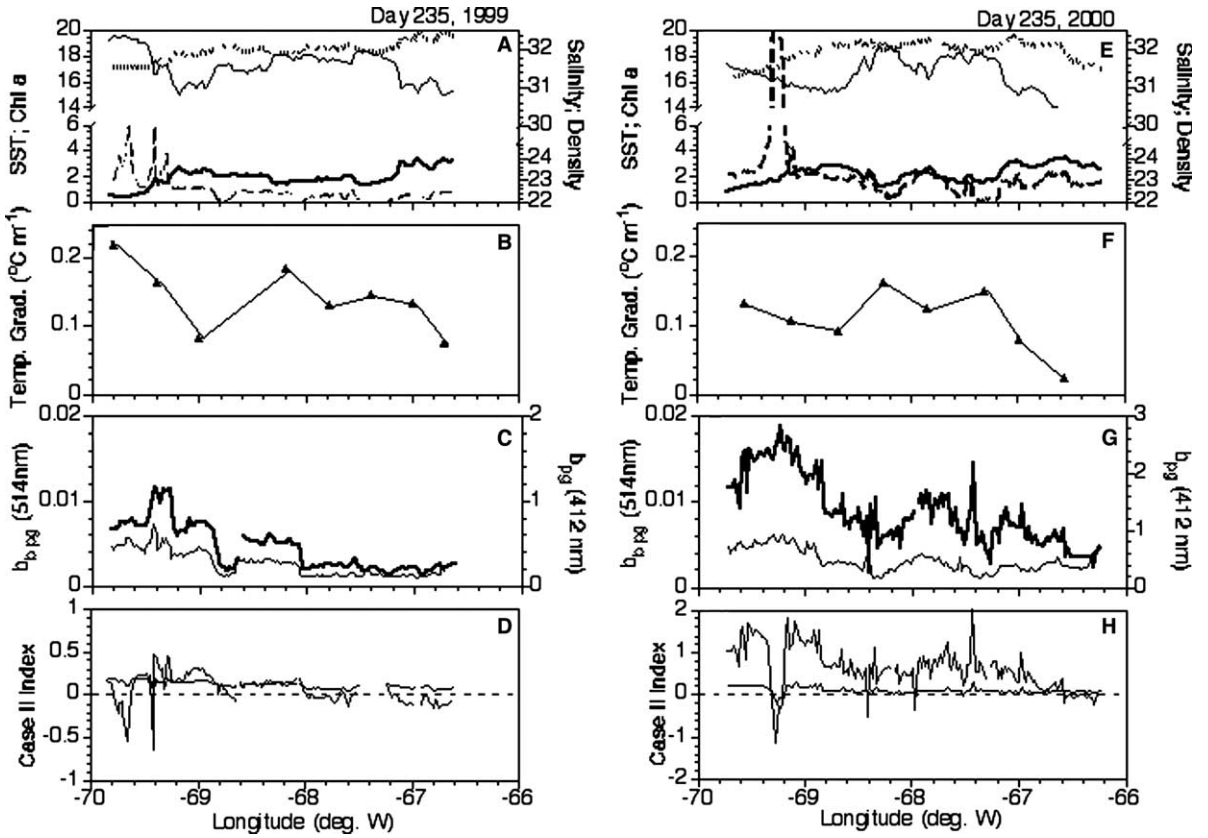

Fig. 4. Examples of Gulf of Maine data from late summer for day 235, 1999 (panels A–D) and day 235, 2000 (panels E–H), all plotted against longitude: Key to different lines same as in Fig. 2.

structure in the density signal observed over spatial scales of 10 km, which was consistent between runs 24 h apart (compare MMC Fig. 8 line K and L, or MMC Fig. 9 line G and H). The cold water observed during fall of 1998 also had lower salinities, such that the density of the 1998 water was similar to the density observed in the other years.

3.6. Vertical temperature gradient and mixed layer depth

The vertical temperature gradient through the top 50 m was least at either end of the transect (<0.04 °C m^{-1}) in late September and October (Fig. 5F and J; MMC Fig. 10 lines H–J; MMC Fig. 11 line S; MMC Fig. 12 line L). Greatest temperature gradients (of $\geqslant$0.16 °C m^{-1}) were usually seen during August and early September (Fig. 4; MMC Fig. 10 line A and B; MMC Fig. 11 line H; MMC Fig. 12 line J). Spatially, weak gradients (<0.04 °C m^{-1}) were observed in SSW near 66.5°W, with maxima >0.16 °C m^{-1} associated with JBW (typically between 67–68.5°W; Figs. 2–5, panels B and F; MMC Figs. 10, 11, and 12). A weakening of the vertical temperature gradient was consistently observed near ~68.5–69°W in the offshore extension of the EMCC, just west of the JBW. Nearer the Maine coast, vertical temperature gradients often increased to 0.16 °C m^{-1}, which occasionally exceeded gradients seen in the Jordan Basin (Fig. 2B, 4B; MMC Figs. 10, 11, and 12).

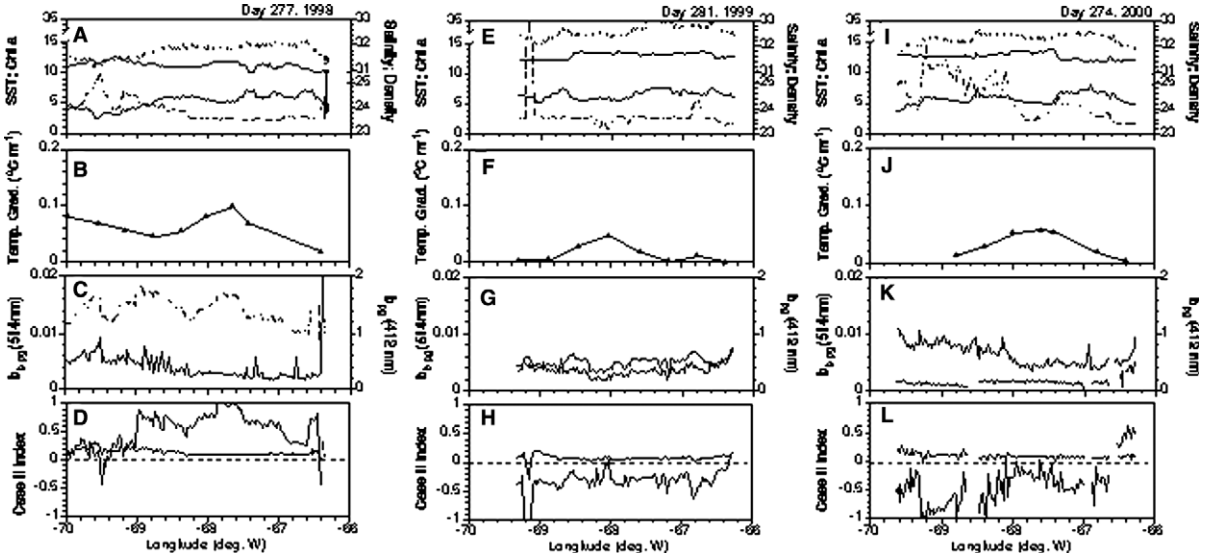

Fig. 5. Examples of Gulf of Maine data from fall day 277, 1998 (panels A–D), day 281, 1999 (panels E–H) and day 274, 2000 (panels I–L), all plotted against longitude: Key to different lines same as in Fig. 2.

Temporally, mixed layer depths were remarkably constant across the Gulf of Maine, with typical values of about 6–8 m during all periods except the fall, when surface cooling and wind-forcing increased the mixing depths significantly (recall that the depth of the mixed layer is defined as the depth at which the temperature deviated >0.1 °C from the uppermost value; MMC Figs.13, 14 and 15). Spatially, the mixed layer was usually deepest in SSW, except during the fall when deep mixed layers could be observed across the entire basin.

3.7. Chlorophyll *a*

Spatial distributions of chlorophyll *a* showed few similarities over the cruises. One commonality was that no high peaks in chlorophyll *a* were ever observed in Jordan Basin; all the peaks were observed on either side of the basin, usually near the frontal boundary separating Jordan Basin from its surrounding water masses (MMC Figs 16–18). Maximum chlorophyll *a* concentrations reached as high as 80 μg chl *a* L^{-1} during the three year study. Such high values were not confined to any particular season, and no relationship was evident between water density and chlorophyll *a* levels. Chlorophyll peaks were observed where vertical temperature gradients were high (Fig. 4A and B), moderate (Fig. 2A,B and E,F; Fig. 3A and B; Fig. 4E and F; Fig. 5A and B) and low (Fig. 5E, F and I, J). Coherency was usually evident in the patterns measured on successive days, but the differences were more notable (e.g., MMC Fig. 16 lines D and E, lines H and I; MMC Fig. 17 lines D–F, lines K–M, lines N and O). While advection cannot be ruled out as causing these differences in the chlorophyll concentration, salinity traces for successive days showed much more coherence than did chlorophyll concentration; this is to be expected, given that chlorophyll *a* is not a conservative tracer as is salinity.

3.8. Interannual variability

For each year of the study, we pooled data into longitudinal bins along the cruise track and calculated bin averages and standard errors (Figs. 6 and 7). We defined surface water mass boundaries based on

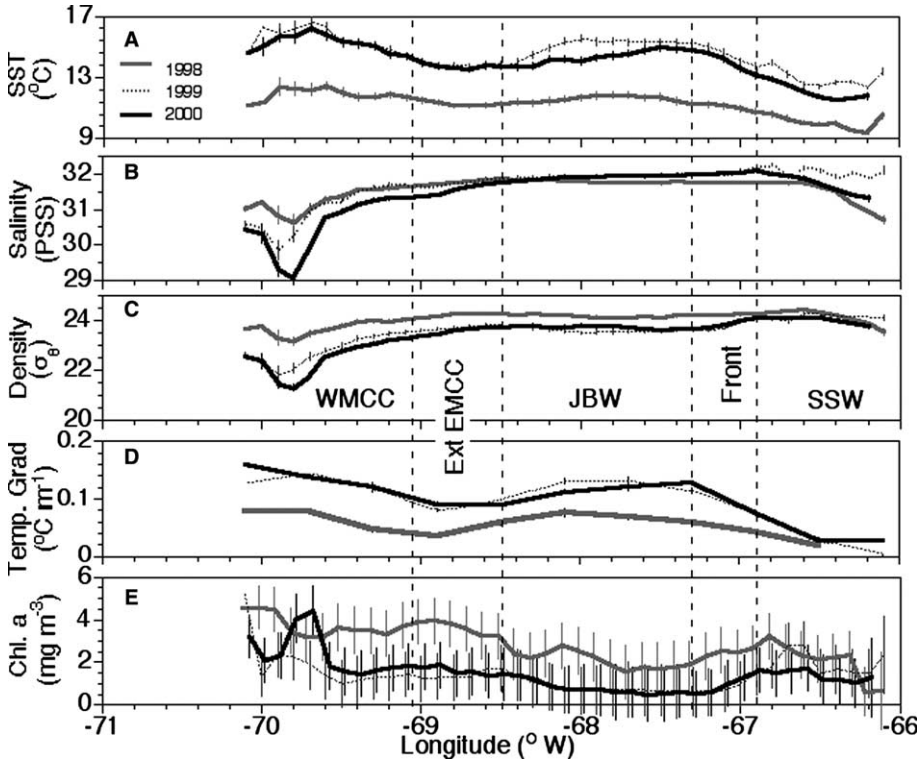

Fig. 6. Plot of mean SST, salinity, density, vertical temperature gradient from 1 to 50 m, and chlorophyll *a* plotted versus longitude. Data for panels A, B, C and E were binned and averaged for each year and for each 0.1° longitude. Data for panel D were binned and averaged for each year and for each 0.4° longitude. The standard error about each mean is shown as a vertical line for each datum. Where the line is not visible, then the standard error is smaller than the actual line used to plot the data. Data points for each year were offset within ±0.02° longitude along the *X*-axis in order that they not overlap and to allow easier viewing. Averages for each year are designated as follows: 1998 – thickest light-grey line; 1999 – thinnest dark-grey line; 2000 – medium thickness black line. Rough positions of various hydrographic water types are designated: Western Maine Coastal Current (WMCC), offshore extension of the Eastern Maine Counter Current (Ext EMCC), Jordan Basin Water (JBW), Scotian Shelf Water (SSW) and the frontal boundary between JBW and SSW (“front”).

density and vertical temperature gradients. Cold temperatures were seen across the entire Gulf of Maine during Fall of 1998. The frontal boundary separating JBW and SSW was centered at 67.1°W (±0.2 °W) (Figs. 2A, 3A, 4A and E, 5I, 6 and 7). SSW generally had reduced salinities near the coast of Nova Scotia (but note, the 3-year maximum in surface salinity was also observed at 66.8°W during 1999, not far off the coast of Nova Scotia). The range in chlorophyll *a* concentrations in the SSW was typically <5.0 μg L^{-1} for a transect but with notably high concentrations, exceeding 15 μg L^{-1}, east of the 67.1°W frontal boundary during 1998 and 1999. Increased SST associated with JBW typically occurred between roughly 67.25°W and 68.6°W (Figs. 6 and 7). The vertical temperature gradient from 1 to 50 m showed strong differences interannually; minimum vertical gradients were consistently seen just off Nova Scotia (<0.05 °C m^{-1}). Moreover, vertical temperature gradients were always greatest in summer months, so that maximum gradients in 1999 and 2000 exceeded those in 1998, when sampling was biased to the fall (Fig. 6D). At the western boundary of the JBW, we frequently passed through offshore extensions of EMCC water that had enhanced chlorophyll *a* concentrations (Fig. 6E). Most frequently, the intrusions occurred between

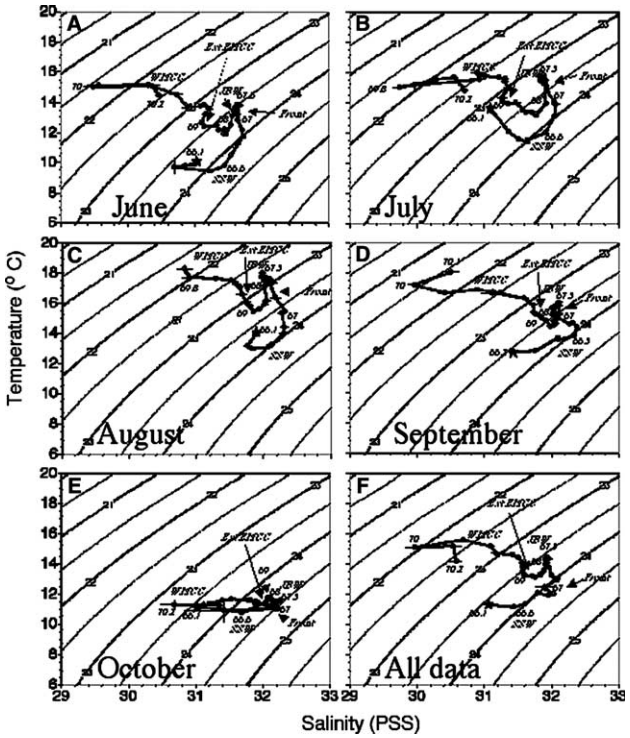

Fig. 7. Temperature versus salinity plots for surface waters, binned for each 0.1° of longitude (~8 km) and averaged for each month of the study. Reference longitudes are shown in italics. Isopleths of density (sigma-theta) are shown for reference. The star in each plot represents the eastern-most value off of Yarmouth, Nova Scotia. Error bars represent one standard error about the mean. If no bar is visible, this indicates that the error bars are smaller than the symbol. Abbreviations are given for the Western Maine Coastal Current (WMCC), the offshore extension of the Eastern Maine Coastal Current (Ext EMCC), Jordan Basin Water (JBW), Scotian Shelf Water (SSW), and the frontal boundary between JBW and SSW.

68.6°W and 69.1°W and were associated with decreases in the vertical temperature gradient and peaks in chlorophyll *a* (up to ~80 μg L^{-1}). The WMCC showed temperature increases with minimum salinities (and densities) from ~69.5 °W to ~70.2°W.

Plots of average monthly temperature-salinity results demonstrated highly reproducible patterns across the Gulf of Maine recurring through the summer and early autumn (Fig. 7). Maximum densities were observed in the SSW and lower densities in JBW. Indeed, JBW was flanked on either side by water of greater density. For June through September, the offshore extension of the EMCC was apparent as a ''bump'' in the *T–S* diagrams. JBW had a density of ~23.5 (sigma-theta units) in June that decreased to ~22.75 in August, then increased to 24.4 in October. The temperature range in October was significantly reduced over the entire transect such that density differences were almost completely driven by salinity (Fig. 7E). Least saline waters were in the WMCC and SSW, while the most dense waters were at the frontal boundary between JBW and SSW. A three-year average by 0.1° of longitude (~8 km) (Fig. 7F) showed the same pattern. One notable difference was a small bend in the *T–S* curve at ~67°W (frontal boundary) which was not present in any of the monthly averages. Given the larger standard error bars associated with just one of the data points, this may be an artifact of data pooling.

The XBT data demonstrated large differences in the water masses within the Gulf of Maine over the three years. Time variability of the volume of MSW showed similar annual patterns, typically accounting

for ~20% of the total volume sampled early-on, increasing to ~50% in the fall (Fig. 8A). MIW was seasonally prevalent during the late Spring but with notable differences over the three years. In fall of 1998, MIW contributed 30–40% of the total volume sampled. During 1999, MIW contributed ~70% of the total volume sampled in early June, decreasing to <10% by 10 August, after which it remained virtually undetectable for the remainder of the sampling period (up to mid-October; Fig. 8B). In 2000, not as much MIW was evident during the spring, and it decreased to ~10% of the total volume sampled by 23 June 2000.

MBW also showed pronounced seasonal variability, with low amounts in the spring (0–30%), increasing over the summer to 75% of the total volume sampled, and decreasing again during the fall to 30–50%. MBW volumes during the fall were lowest in 1998. The earliest influx of MBW was observed during 2000, beginning about calendar day 164 (Fig. 8C). Individual sections of temperature show intrusion events near the bottom on the eastern side of the transect (Fig. 8D–I).

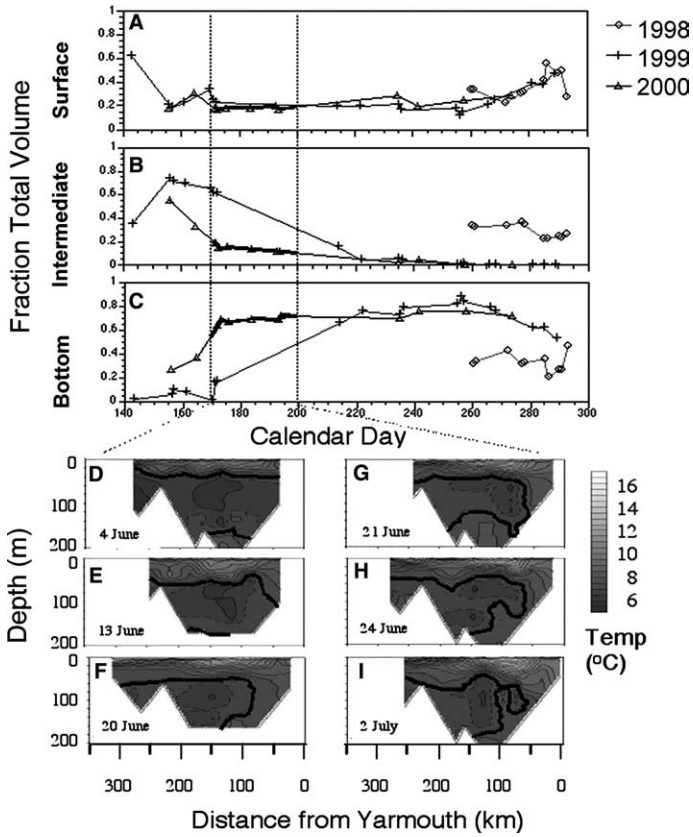

Fig. 8. Results of XBT analyses, showing the fraction of surface water, intermediate water and bottom water observed during each cruise: (A) fraction volume contributed by Maine Surface Water, (B) fraction volume contributed by Maine Intermediate Water and (C) fraction volume contributed by Maine Bottom Water. See text for temperature criteria for defining these water types. Heaviest lines in panels A–C refer to data used to make vertical temperature sections shown in panels D–I. These vertical cross sections were from a 29-day period during the year 2000 when there were 6 ferry trips (the time period falls between the two vertical dashed lines in panels A–C). Temperature sections are shown from 4 June (cal. day 156), 13 June (cal. day 165), 20 June (cal. day 172), 21 June (cal. day 173), 24 June (cal. day 176), and 2 July (cal. day 184). During this period, North Atlantic slope water appears to have moved into the Gulf of Maine on the western side of Jordan Basin as indicated by strong vertical deflection of isotherms beginning on 20 June 2000, from ~80 m depth to the bottom. The dashed line indicates the 7 °C isotherm and the heavy black line indicates the 8 °C isotherm in all sections.

The temperature gradient from 1 to 50 m was significantly, negatively correlated to the surface density (Gradient = $-7.334 \times 10^{-2} * \sigma_{\theta\ \text{surface}} + 1.830$; $r^2 = 0.592$; $n = 325$; $P < 0.001$; Fig. 9). Moreover, the mean cruise-wide surface density was significantly correlated to the amount of MSW observed in the XBT sections (Fig. 10A; Mean $\sigma_{\theta\ \text{surface.}} = 7.106 \times 10^{-8} *$ MSW cross-sectional area + 23.13; $r^2 = 0.443$; $n = 41$;

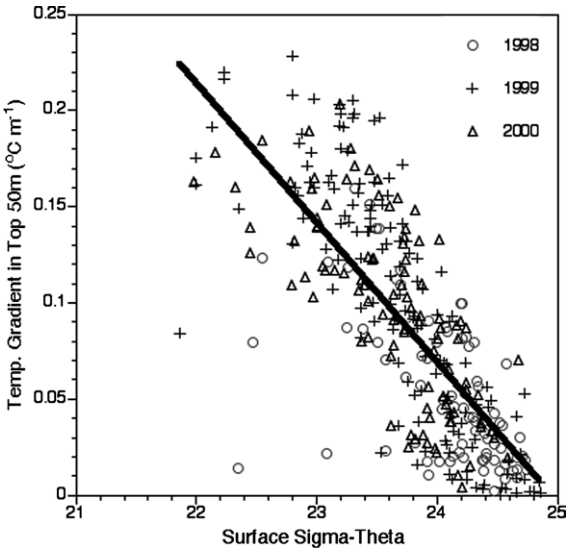

Fig. 9. Average vertical temperature gradient from 1 to 50 m (°C m^{-1}) versus surface σ_θ for all cruises. Symbol key given in the upper right of the figure. The line represents the least-squares fit to the three years of observations. The statistics of the fit are given in the text.

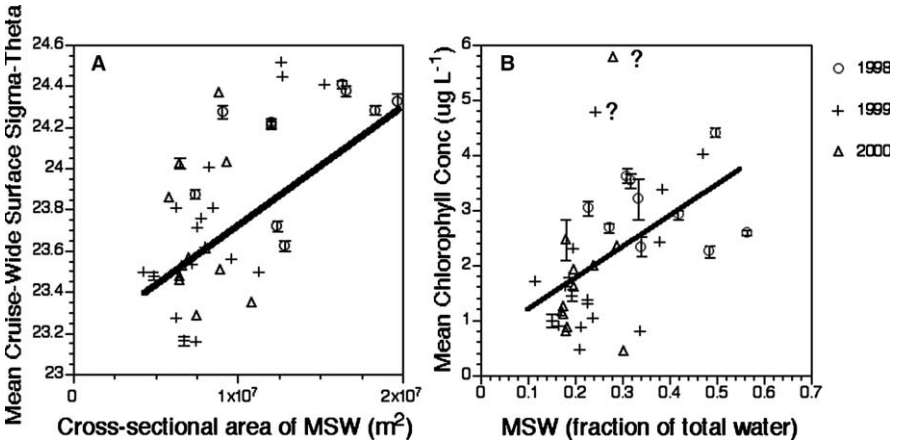

Fig. 10. (A) Mean cruise-wide surface σ_θ versus cross-sectional area of Maine Surface Water (MSW; m^2) estimated from XBT profiles. Least-squares fit to data is shown by the black line. The regression for the data is: $\sigma_\theta = 7.106 *$ MSW + 23.127; $r^2 = 0.443$. (B) Mean cruise-wide chlorophyll *a* concentrations plotted against the amount of Maine Surface Water (shown as a % of the total water surveyed). Error bars represent standard errors. Linear regression equations have been defined for the entire data set ($Y = 5.118 * X + 0.640$; $r^2 = 0.251$; not shown on figure) and for the data set with two outliers removed ($Y = 5.911 * X + 0.382$; $r^2 = 0.400$; black line shown in panel). Symbol key given on the upper right of panel A.

$P < 0.001$). With the exception of two outlier cruises, the gulf-wide mean chlorophyll concentration was also significantly correlated with the amount of MSW (mean chlorophyll $a = (0.591 \times (\text{fraction of total water occupied by MSW})) + 0.382$; $n = 40$; $r^2 = 0.40$; $n = 38$; $P < 0.001$; Fig. 10B).

3.9. Light scattering

Optical variability showed moderate correspondence with the water mass boundaries. Total backscattering at 514 nm and total scattering at 412 nm demonstrated coherent peaks (Figs. 2C, 3C and G, 4C and G, 5C and G). Nonetheless, there was less coherence between peaks in $b_{\text{b pg 514}}$ and chlorophyll (MMC Figs. 19, 20 and 21 versus MMC Figs. 16, 17 and 18, respectively). A few examples of coherent peaks were seen in the cruises from July 11 and 12, 2000 (compare Fig. 2E–G; Fig. 4A–C; Fig. 5A–C; MMC Fig. 21 to MMC Fig. 18, lines G and H in both figures). Overall, optical backscattering showed more evidence of fine-scale patchiness than did chlorophyll *a* (Fig. 2A vs. C).

Acid-labile backscattering provided an indication of how much suspended calcium carbonate from coccoliths was present. Negative values occasionally resulted from the fact that a single instrument was measuring both total and acidified backscattering, sequentially within each 4 min period. If a rare, large, particle went through the light scattering photometer during the acid cycle, or if the ship was passing through a steep gradient in particulate backscattering, then mean $b_{\text{b pg acid}}$ could exceed $b_{\text{b pg}}$, leading to a negative b'_{b}. Such negative values usually were not significantly different from zero. Overall, acid-labile backscattering showed strong patchiness. In year 2000, small peaks in acid-labile backscattering were observed at about 67.2–67.3°W (e.g., between June 13 and 20; MMC Fig. 24). By 21 June, a significant peak of $3–4 \times 10^{-3}$ m^{-1}, about 30 km wide, was centered at ~67.3°W (MMC Fig. 24 line D). From 24 June to July 2, 2000, a broad region of significantly positive b'_{b} ($>2 \times 10^{-3}$ m^{-1}) stretched completely across Jordan Basin, between ~66.7°W and 68.3°W (Fig. 3G; MMC Fig. 24 lines E and F), with highest values where vertical temperature gradients were decreasing from the greatest values in JBW (MMC Fig. 12 lines E and F). A similar pattern was seen on 11 July 2000 (MMC Fig. 24 line G). On 14 September, water with significantly positive b'_{b} ($2–3 \times 10^{-3}$ m^{-1}) was observed in the Western Gulf of Maine (MMC Fig. 24 line K).

We also examined acid-labile backscattering as a percentage of the total particulate and dissolved backscattering at 514 nm. A common attribute of the individual transects was a large peak in the $b'_{\text{b 514}}/b_{\text{btot 514}}$ ratio just off Yarmouth, NS (MMC Fig. 26). The patterns during September/October 1998 showed a high degree of patchiness in $b'_{\text{b pg 514}}/b_{\text{b pg 514}}$ with little discernable pattern (e.g., MMC Fig. 25). The same applied to late spring/early summer in 1999, when occasional peaks approaching 100% were observed, but with little coherence with any of the other hydrographic boundaries (MMC Fig. 26, lines A–F). From August through mid-September, 1999, the $b'_{\text{b pg 514}}/b_{\text{b pg 514}}$ ratio was typically about 10–20% with an occasional peak of 30% (MMC Fig. 26, lines G–M). From 24–25 September, 1999, the ratio across Jordan Basin increased to 20–30% (MMC Fig. 26, lines M and O). For the remaining October 1999 cruises, values had a range of 0–30% (mostly 10–20%), showing a high degree of patchiness (MMC Fig. 26 lines P–R). Finally, during 2000, the same high degree of patchiness was seen during the late spring/early summer, with little coherence between cruises, even from day to day (e.g., MMC Fig. 27 lines A–D). Between 20 June and 12 July, 2000, however, a bloom of coccolithophores developed across the Jordan Basin, and $b'_{\text{b pg 514}}/b_{\text{b pg 514}}$ values of 30–70% were consistently observed (Fig. 3G; MMC Fig. 27 lines E–H). This bloom was confirmed microscopically and was visible from SeaWiFS and MODIS-Terra (Balch, 2004). The bloom gave way to highly patchy distributions through August and September of 2000 with values of 10–20% (MMC Fig. 27 lines I–L).

When data from each year were binned and averaged, backscattering of particulate and dissolved material at 514 nm showed an order of magnitude variability among the 3 years of sampling (Fig. 11). The spatial distribution of particulate backscattering at 514 nm showed highest values approaching the coast in either SSW or the WMCC (Fig. 11A). JBW had the lowest values of $b_{\text{b pg 514}}$, ranging from

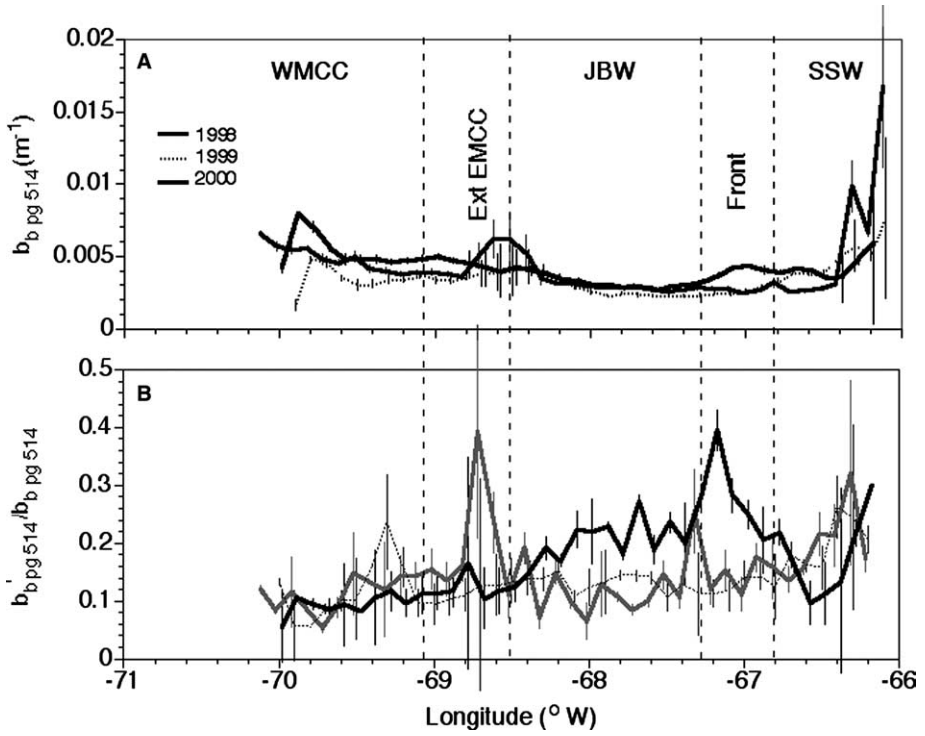

Fig. 11. Three years of surface Gulf of Maine backscattering measurements versus longitude, taken from *M/S Scotia Prince* ferry: (A) total particle and detrital backscattering in surface water ($b_{b\,pg\,514\,nm}$; water subtracted), (B) fraction of $b'_{b\,pg\,514\,nm}/b_{b\,pg\,514\,nm}$. Data for each year were binned and averaged within each 0.1° longitude (~8 km) increment. Vertical error bars represent one standard error about each mean. Data points for each year were offset by ±0.02° longitude along the *X*-axis in order that they not overlap. Approximate boundaries between Western Maine Coastal Current (WMCC), the offshore extension of the offshoreEastern Maine Coastal Current (EMCC Ext), Jordan Basin Water (JBW) and Scotian Shelf water (SSW) are designated with dashed lines. A key for the line colors and weights is given in panel A.

0.001–0.006 m^{-1}. Values >0.01 m^{-1} were reported at the frontal boundary between JBW and SSW during 2000 (Fig. 2G).

Acid-labile backscattering estimates (MMC Figs. 22–24) typically were between 0 and 0.002 m^{-1}; negative values usually were not significantly different from zero. The average $b'_{b\,pg\,514}$ for the entire three-year series was 1.72×10^{-3} m^{-1} (SE ± 3.372×10^{-5}; $n = 4609$). Interannual variation also was seen in $b'_{b\,pg514}$. For example, the 2000 data set showed greater values of b'_b than the1998 and 1999 seasons with the majority of zero values observed in the WMCC. Moreover, based on the binned, average data, much of the added b_{bp} at the frontal boundary between the JBW and SSW water (Fig. 11A) was acid-labile (Fig. 11B), and was later confirmed microscopically to be populations of the coccolithophore, *E. huxleyi*.

Binned and averaged acid-labile backscattering values demonstrated significant increases above background for all three years near the coast of Nova Scotia, just as expected from the individual cruise traces. Fig. 11B shows $b'_{b\,pg\,514}/b_{b\,pg\,514}$ along the cruise track. Values of $b'_{b\,pg\,514}/b_{b\,pg\,514} = 25\%$ were common in JBW while in the EMCC, $b'_{b\,pg\,514}/b_{b\,pg\,514}$ was usually 10–20%. For the 2000 *E. huxleyi* bloom at the JBW/SSW frontal boundary, values of $b'_{b\,pg\,514}/b_{b\,pg\,514}$ reached 60–80% (Fig. 11B; MMC Fig. 27 line E and F). The 2000 data overall showed a greater decrease in scattering following acidification than in other years. Values of $b_{b\,pg\,acid\,514}$ were significantly correlated with $b_{b\,pg\,514}$ and the average least-squares relation was: $b_{b\,pg\,acid\,514} = 0.529 \times b^{0.899}_{b\,pg\,514}$ ($r^2 = 0.755$; $n = 6647$; $P < 0.001$; Fig. 12).

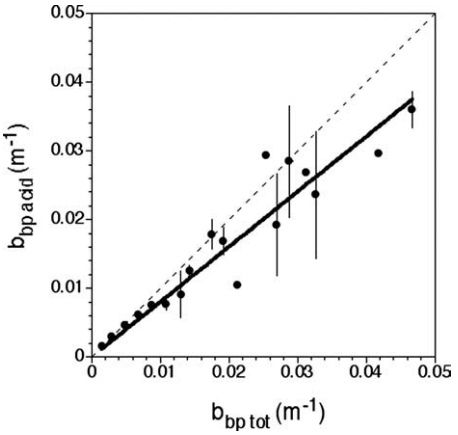

Fig. 12. Acidified particulate backscattering versus total particulate backscattering (both at 514 nm) for three years of ferry sampling. Data for this figure were binned and averaged every 0.002 m^{-1}. Error bars represent ±one standard deviation. Error bars are only shown in the *Y* direction because the *X* data were binned (required in order to simplify the presentation of thousands of data points). The reader should note, however, that the same instrument was used to make both measurements. Thus, for the same values of acidified particulate backscattering or total particulate backscattering, the experimental errors should have been similar. Least-squares fit to entire data set is shown as the solid line. The regression for this fit is: $b_{bp\,acid\,514} = 0.803 * b_{bp\,514}$; $r^2 = 0.896$. A 1:1 dashed line is shown for reference.

Light scattering by particulate and dissolved material at 412 nm (excluding water) typically varied between 0 and 2 m^{-1} across the transect (e.g., panels C and G of Figs. 2–5), with values that decreased away from the coast of Nova Scotia, towards the boundary with the JBW (MMC Fig. 28). Elevated scattering was observed across the Gulf of Maine in early August, 1999 (MMC Fig. 29 lines G and H) which gave way to elevated scattering, mainly in the western Gulf of Maine from late August to mid-September (MMC Fig. 29 lines I–L). This abruptly changed on 14 September 1999 when high values again prevailed across the Gulf (MMC Fig. 29 lines M and N). The 412 nm scattering showed several coherent peaks for 3 weeks, between 24 August 1999 and September 13, 1999 (e.g., MMC Fig. 29 lines J–L), with peaks near 69.4°W, 68.6°W and 66.75°W. Regions with consistently high $b_{pg\,412}$ were seen again during 2000 (e.g., MMC Fig. 30 line I).

In year 2000, we began observations of dissolved (<0.2 μm filtered) spectral scattering. The results demonstrated typical $b_{g\,412}$ variability of 0–0.3 m^{-1} with several large areas with 0.8–1.4 m^{-1} (MMC Fig. 31, lines B, C, and I). For most of the trips in 2000, the western GOM values were higher than Jordan Basin values (MMC Fig. 31 lines E–K). Using averaged data, it can be seen that within the Jordan Basin, average $b_{pg\,412}$ showed a 2-fold variation over the three years, still lower than in the coastal SSW. Levels of $b_{g\,412}$ in the Jordan Basin were moderate, and showed no discernable trend from east to west. In the WMCC, both $b_{pg\,412}$ and $b_{g\,412}$ increased towards the coast, with the scattering for <0.2 μm particles showing the most obvious increase with decreasing salinity off the Maine coast (Figs. 6B and 13B).

Backscattering probability at 514 nm ($\tilde{b}_{b514}$) was typically less than 1%, but there was obvious patchiness visible along the cruise track (MMC Figs. 32–34). In situations of high suspended calcium carbonate, peaks in $\tilde{b}_{b\,514}$, aligned with peaks in $b'_{b\,pg\,514}$ and $b'_{b\,pg\,514}/b_{b\,pg\,514}$ (e.g., day 176, 2000; MMC Figs 24, 27 and 34, line E), but outside the coccolithophore features, the $\tilde{b}_{b\,514}$ ratio appeared to show significant variability driven by other types of particles. Near the summer solstice of 1999 (MMC Fig. 33 line G) and 2000 (MMC Fig. 34 line E), $\tilde{b}_{b\,514}$ decreased westward across the transect with lowest values in the WMCC. This trend reversed

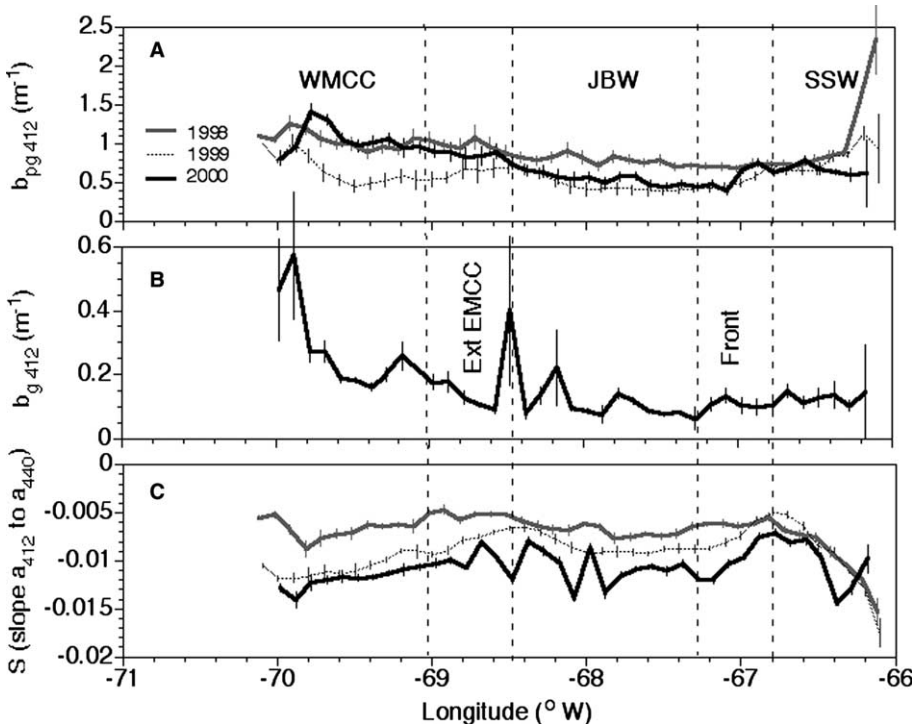

Fig. 13. (A) Particle and detrital scattering ($b_{pg\,412\,nm}$; water subtracted) versus longitude. (B) Scattering by <0.2 μm fraction ($b_{g\,412\,nm}$) versus longitude. Data for each year were binned and averaged within each 0.1° longitude (~0.8 km) increment. Vertical error bars represent one standard error about each mean. Data points for each year were offset by ±0.02° longitude along the *X*-axis in order that they not overlap and to allow easier viewing. Approximate boundaries between Western Maine Coastal Current (WMCC), the offshore extension of the offshoreEastern Maine Coastal Current (EMCC Ext), Jordan Basin Water (JBW) and Scotian Shelf water (SSW) are designated with dashed lines. A key for the line colors and weights is given in panel A.

by early October, with highest $\tilde{b}_{b\,514}$ values in the WMCC (MMC Fig. 33, line Q). During other periods, cross-Gulf trends in $\tilde{b}_{b\,514}$ were not evident.

Particulate backscattering, measured with the Hydroscat-2, was compared to particulate backscattering measured with the Wyatt Technology instrument. Only data from 1999 and 2000 were available for this comparison. The Hydroscat 2 data at 470 and 676 nm were interpolated in order to estimate the 514 nm value. The interpolation assumed backscattering increases as the wavelength raised to a power (Mobley, 1994). The results (Fig. 14) approximately center about the 1:1 line, especially for waters with higher backscattering levels; however, it is important to point out the significant standard deviations of the binned data. The best-fit relationship between the two instruments was: $b_{b\,pg\,514\,HOBI} = 0.19(b^{0.715}_{b\,pg\,514\,Wyatt})$ [$r^2 = 0.423$; $n = 3029$; $P < 0.001$]. Comparisons between volume scattering as measured by the HOBI Labs Hydroscat and Wyatt Technology instruments, at the same angles, have been published elsewhere (Vaillancourt, Brown, Guillard, & Balch, 2004). Some of the difference can indeed be ascribed to the shape of the VSF implicitly assumed in the HOBI Labs instrument.

3.10. Variability in the shape of the volume scattering function

We observed a clear difference in VSF shape in the Gulf of Maine as compared to the classic VSF shape for coastal waters, originally described by Petzold (1972)(Fig. 15A). At 45°, we consistently saw

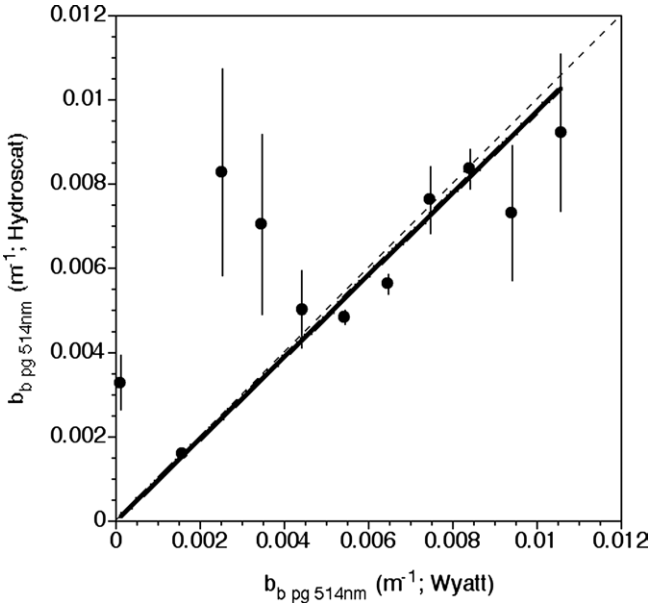

Fig. 14. Particulate backscattering estimated from measurements by Wyatt Dawn-F light scattering photometer versus that estimated by HOBI Labs Hydroscat II. Data for this figure were binned and averaged every 0.001 m^{-1}. Error bars represent ±one standard deviation. Least-squares fit to entire data set is shown as the solid line. The 1:1 line (dashed line) is shown for reference and the least-squares fit for all three years of data is shown as a heavy black line ($Y = 0.9716X$; $r^2 = 0.491$). Note, both Dawn and Hydroscat II data had experimental error but due to the statistical binning (required to simplify the number of data points for presentation here), only confidence intervals for the Hydroscat II data are shown for each range of Wyatt Dawn-F values.

values of $\beta_{\text{norm}\,45}$ that were 65–95% of Petzold's values ($\beta^{45}_{\text{norm Petzold Interp}}$). Moreover, the forward-angle scattering showed coherent changes through the seasons, over all three years, with peak values during the summer, and lower values during spring and fall (Fig. 15B). At 135°, the Gulf of Maine normalized volume scattering was usually ~25–50% greater than Petzold's and there was no coherent temporal variability throughout the spring, summer or fall (Fig. 15C). Examination of the fall data for the three years revealed interannual variability; cruise means for 135° normalized scattering were 127%, 126% and >150% of Petzold's values in 1998, 1999 and 2000, respectively. Cruise means for 2000 were significantly higher than in 1999. Normalized volume scattering functions showed little spatially-coherent variability, and variance at 45° and 135° only increased at the frontal boundary between JBW and SSW (Fig. 16; here we averaged all 3 years of data). Normalized volume scattering from the SSW showed that the mean $\beta_{\text{norm}\,135}$ decreased from 135–140% of Petzold's coastal water values (observed for virtually the entire transect), to values of 125% near the coast of Nova Scotia (Fig. 16). Average volume scattering values have been compiled for all three years of data and are presented in Table 2.

3.11. Absorption by dissolved organic matter

Absorption at 412 nm showed clear peaks west of 68.5°W during periods lasting up to several weeks (MMC Fig. 35A–F, MMC Fig. 36J–N, MMC Fig. 37G–L). Minima in 412 nm absorption were usually in the JBW, and slight increases were often seen in coastal SSW (MMC Figs. 35–37). The slope of the absorption between 412 and 440 nm showed the least negative values at the frontal boundaries on either side of Jordan Basin (MMC Figs. 38–40). Moreover, the JBW often had more negative absorption slopes. (e.g., see MMC Fig. 39J–L; MMC Fig. 40G and H).

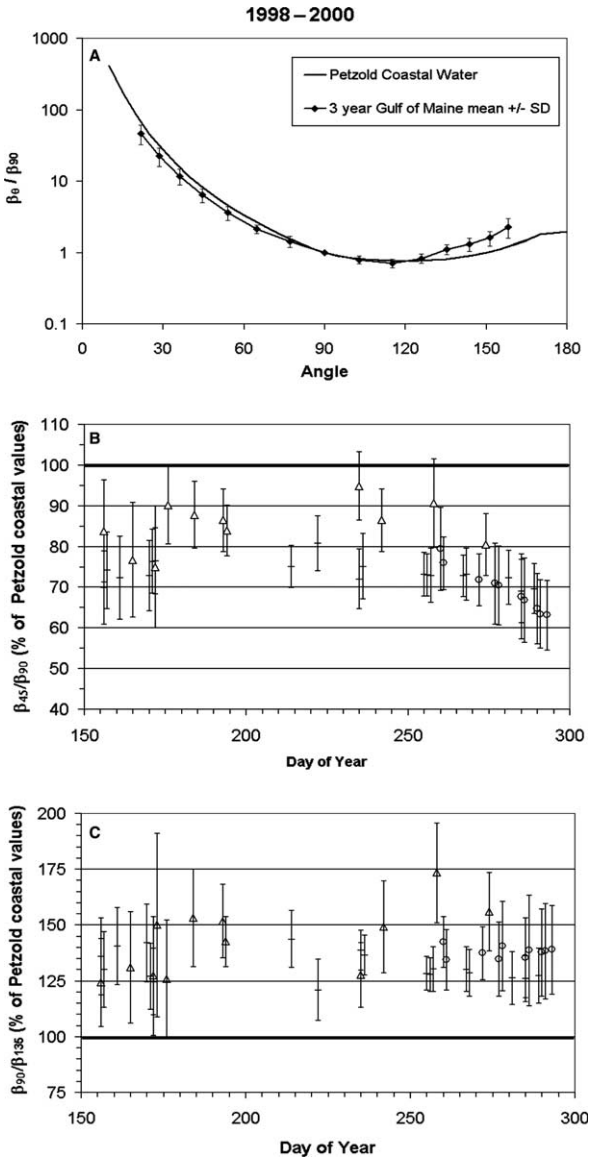

Fig. 15. (A) Three-year averages of normalized volume scattering at 45° as a fraction of Petzold normalized volume scattering at 45° (Petzold, 1972). Each point on the plot is an average of 6766 spatially-integrated samples from our underway system in which each sample consisted of 10,000 individual backscattering measurements. Error bars represent one standard deviation about the mean. Petzold's data for coastal waters (Petzold, 1972) are shown for comparison (heavier black line). (B) Time variability in shape of volume scattering function. Each point represents a cruise-wide mean and the error bars represent one standard deviation about the mean. A value of 100% on the *Y*-axis means that the normalized volume scattering at 45° is the same as predicted by Petzold (1972). Symbols designate different years: O = 1998, + = 1999, Δ = 2000. (C) Same as in panel A, but for normalized volume scattering at 135°.

3.12. Observations of Case I and II waters

The presence of Case I and Case II waters for suspended particulate matter in the Gulf of Maine was investigated by comparing our 550 nm scattering data to the expected scattering data based on the

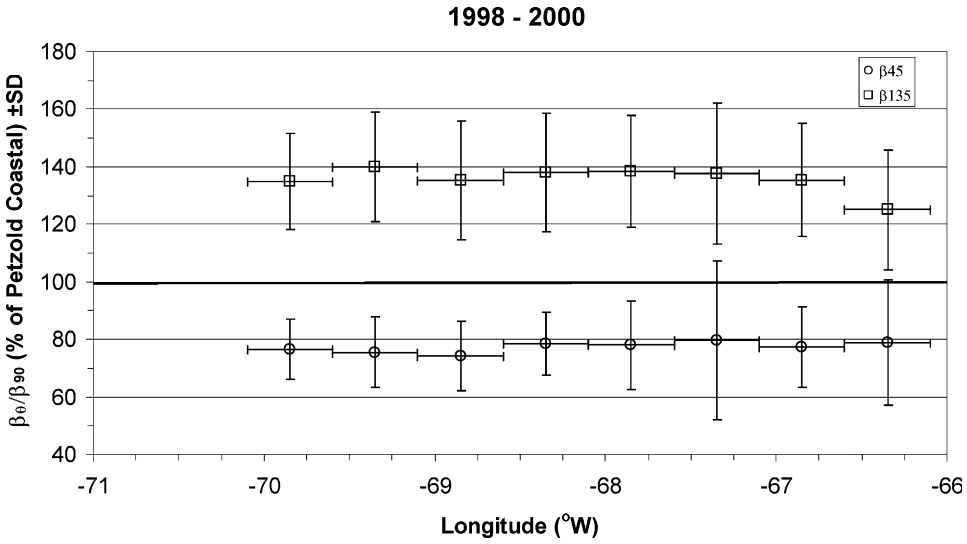

Fig. 16. Spatial variability in normalized 45° and 135° volume scattering for three years of sampling within the Gulf of Maine from the *M/S Scotia Prince* ferry. Each point represents the mean volume scattering (normalized to 90° and expressed as a percentage of the normalized Petzold (1972)) for all cruises, within a 0.5° longitude range. Vertical error bars represent one standard deviation about the mean.

Table 2
Average volume scattering function at 514 nm for Gulf of Maine samples presented in absolute terms (m^{-1} sr^{-1}) and normalized to the 90° value (unitless)

Angle (deg)	β_θ	SD	SE	$\beta_\theta/\beta_{90}°$	SD	SE
21.7	0.02067	0.006097	7.44921E − 05	46.39244	14.29633	0.174658
28.7	0.012112	0.005333	6.51501E − 05	22.28083	6.313149	0.077127
36.1	0.005888	0.002134	2.60702E − 05	11.63722	2.918003	0.035649
44.5	0.00364	0.001768	2.16035E − 05	6.39411	1.378377	0.01684
54	0.002051	0.001005	1.22729E − 05	3.603214	0.802533	0.009805
64.9	0.001226	0.000619	7.56317E − 06	2.128134	0.304372	0.003719
77.1	0.00082	0.00042	5.12957E − 06	1.429893	0.24953	0.003048
90	0.000578	0.000289	3.52552E − 06	1	0	0
102.9	0.000454	0.000231	2.82746E − 06	0.785411	0.096209	0.001175
115.1	0.000406	0.000204	2.48943E − 06	0.70213	0.092708	0.001133
126	0.000474	0.00024	2.93509E − 06	0.825948	0.127759	0.001561
135.5	0.000619	0.000276	3.36918E − 06	1.104226	0.16898	0.002064
143.9	0.000728	0.000322	3.93111E − 06	1.309529	0.280866	0.003431
151.3	0.000883	0.000384	4.68935E − 06	1.600026	0.368997	0.004508
158.3	0.001269	0.000648	7.91887E − 06	2.283493	0.712067	0.008699

A total of 6700 means (each based on 50 s of measurements at 250 Hz) were used to derive these statistics.

concentration of chlorophyll *a*. The boundary in particle scattering, above which waters were considered Case II for particulate matter, was defined according to Morel (1980) and Gordon and Morel (1983). They derived a mean relationship based on their large surveys between chlorophyll *a* concentration (C) and expected 550 nm scattering($b_{550\,\mathrm{expected}}$):

$$b_{550\,\mathrm{expected}} = 0.45C^{0.62}. \quad (1)$$

When observed 550 nm scattering exceeded the expected mean chlorophyll-dependent scattering, the water was considered Case II for particulate matter (hereafter labeled Case $\mathrm{II}_{\mathrm{partic}}$). Within our data

set, the least-squares power fit between b_{555} (1983; 1980) versus chlorophyll concentration was: $b_{pg\,555} = 0.513\ C^{0.32}$ ($n = 5763$, $r^2 = 0.305$; $P < 0.001$), less steep than the relationship in Eq. (1) but the Gulf of Maine data nonetheless overlap the line defined by Eq. (1). The value of the constant in the Gulf of Maine relationship (0.513) was not significantly different from the constant in Eq. (1), but the exponent (0.32) was significantly lower than that in Eq. (1) ($P < 0.01$; this test was based on a linear transformation of the model relationship (Eq. (1)) followed by an analysis of variance of similarly-transformed data, tested against the linearized model). Note, the wavelength of our scattering measurements was 5 nm greater than the wavelength used by Morel (1980) and Gordon and Morel (1983), but this would have had a negligible effect on the results.

Results for the individual cruises showed that the GOM had periods in which it was mostly Case II_{partic} (e.g., 9/17/98 to 10/5/98; MMC Fig. 41 lines A–E; Fig. 5D) which then gave way to predominantly Case I particulate conditions from 10/12/98 to 10/20/98 (MMC Fig. 41 lines F–J). For 1999, the waters were Case II_{partic} through 13 September (Figs. 3D,4D; MMC Fig. 42 lines A–L), although between 6 and 21 June, 1999, the waters at 66.7°W consistently showed a minimum in the Case II_{partic} index (MMC Fig. 42 lines B-F; Fig. 3D). With few exceptions, during 2000, waters were Case II_{partic} over much of the transect. Only during a cruise late in the year (30 September 2000) was the GOM mostly Case I for particulate material (MMC Fig. 43 line L; Fig. 5L). Plotted together, the data demonstrate that the surface waters along the ferry track could be considered Case II_{partic} about half the time but with few consistent east-west trends (MMC Figs 41–43). Only in 2000 did the waters show a general increase in the Case II_{partic} index from east to west (Fig. 17A). As with scattering and backscattering, SSW waters, EMCC offshore extension and WMCC waters had sporadic peaks in Case II_{partic} conditions. It is also worthy of note that surface waters of Jordan Basin were Case II_{partic} about half of the time.

We also examined the optical data for indications of Case II water for dissolved and detrital material. This was done by calculating the expected total 412 nm absorption for Case I waters using the observed chlorophyll *a* concentration as input to equation 3.27 from Mobley (1994), originally based on Morel (1991) and Prieur and Sathyendranath (1981):

$$a_{tot}(\lambda) = [a_w(\lambda) + 0.06ac^{*\prime}(\lambda)C^{0.65}][1 + 0.2\exp(-0.014(\lambda - 440))], \quad (2)$$

where C is the chlorophyll *a* concentration (mg m^{-3}), $a_{tot}(\lambda)$ is the total absorption at wavelength λ, and the constants $a_w(\lambda)$ and $ac^{*\prime}(\lambda)$ are 0.017 m^{-1} and 0.828 m^2 [mg chl]$^{-1}$, respectively (values for 410 nm taken from Table 3.7 of Mobley (1994)). Eq. (2) predicts $a_{tot}(\lambda)$, which is equal to pure water absorption plus the absorption of particulate and dissolved material ($a_{tot}(\lambda) = a_{pg}(\lambda) + a_w(\lambda)$). However, our field measurements were of only $a_{pg}(\lambda)$. Thus, we added known $a_w(\lambda)$ values to our $a_{pg}(\lambda)$ results so that we could compare field $a_{tot}(\lambda)$ estimates with those predicted from Eq. (2). When observed $a_{pg\,412}$ exceeded that predicted by Eq. (2), then the waters were considered Case II dissolved (Case II_{diss}). It is important to emphasize that our approach was to predict the threshold $a_{pg}(\lambda)$, above-which waters would be considered Case II for colored dissolved *and* detrital organic matter. This approach cannot be used to generate a criterion to predict Case II waters for only colored dissolved organic matter, however. Ideally, CDOM contains only truly dissolved organic matter, but the definition of CDOM is ambiguous in that it includes both particles and dissolved material that passes a <0.2 μm filter. In short, given that there is a continuum of dissolved material plus particles in the range of 0.2–4 μm that are detrital in origin (such as organic aggregates/colloids/polymer gels; Chin, Orellana, & Verdugo, 1998; Koike, Hara, Terauchi, & Kogure, 1990; Wells, 1998), we have chosen to examine $a_{pg\,412}$ here, relative to those values expected in Case I waters (after subtraction of water absorption, of course).

Gulf of Maine $a_{pg\,412}$ values almost always exceeded those predicted by Eq. (2), often by 0.2–0.5 m^{-1}. This suggests that the surface waters of the Gulf of Maine are almost always Case II_{diss} (Figs. 2–5, 17B; MMC Figs 44–46). Not surprisingly, our results clearly show that the WMCC had the

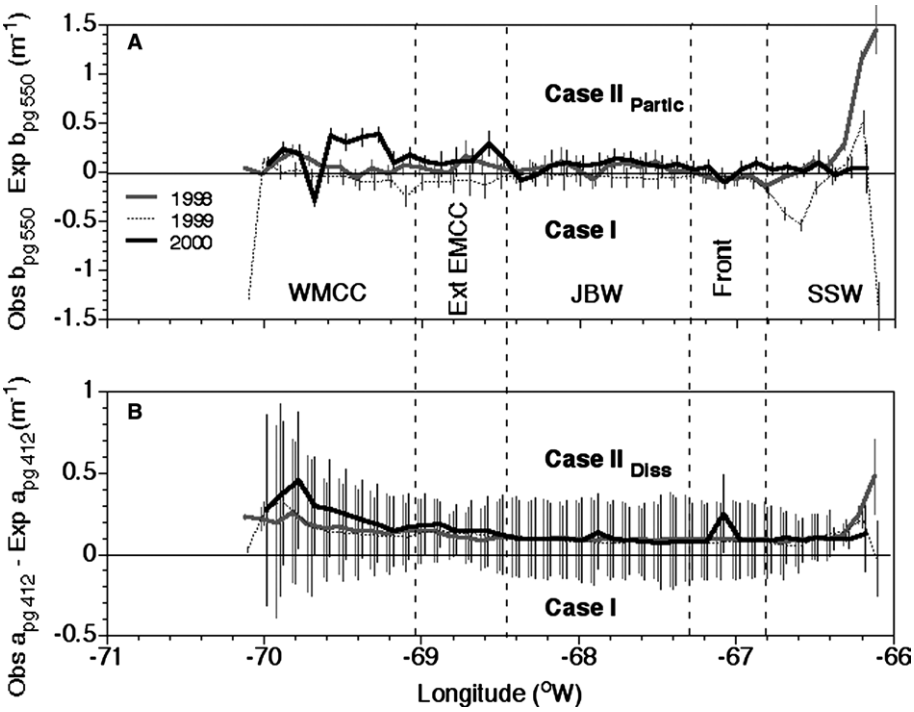

Fig. 17. Spatial variability in indices for (A) Case II_{partic} water and (B) Case II_{diss} water for surface samples taken from the *M/S Scotia Prince* ferry. Key for line colors and weights is given in panel A. Data for each year were binned and averaged within each 0.1° longitude (~0.8 km) increment. Vertical error bars represent one standard error about each mean. Data points for each year were offset by ±0.02° longitude along the *X*-axis in order that they not overlap. Approximate boundaries between WMCC, EMCC Ext, JBW and SSW are designated with dashed lines. See text for details on calculation of the indices. Negative values represent Case I water and positive values represent Case II_{partic} or Case II_{diss} water, respectively.

highest levels of dissolved and detrital absorption, followed by the EMCC offshore extension, then Jordan Basin (Fig. 17B). There does appear to be another source of CDOM and detritus near the coast of Nova Scotia as evidenced by higher $a_{pg}(\lambda)$ values close to shore (Fig. 5H; MMC Fig. 44G–J; MMC Fig. 45K–P; MMC Fig. 46F).

4. Discussion

4.1. Spatial variability

These results demonstrate that the high chlorophyll *a* concentrations across our cruise track were not associated with particular times in summer and early autumn, nor were they associated with intrusions of high-density seawater (either vertically, from deeper in the water column, or horizontally from outside the survey area) which presumably would have contained higher nutrient concentrations. This conclusion is based on the observation that waters with closely similar density structure showed very different ranges in chlorophyll concentration. For example, on day 281, 1999, the range of chlorophyll *a* was <1–30 μg L^{-1} over the transect (Fig. 2; MMC Figs. 8 and 17 line P) but four days later on day 285, 1999, the range of chlorophyll *a* concentration observed over the transect was 1–4 μg L^{-1} (MMC Figs. 8 and 17 line Q). High chlorophyll *a* concentrations were consistently observed in association with

specific hydrographic discontinuities, such as the frontal boundary associated with the EMCC offshore extension, or the tidal front associated with the transition between SSW and JBW (Pingree, Pugh, Holligan, & Forster, 1975; Simpson & Hunter, 1974) (Fig. 6). High chlorophyll concentrations on the eastern end of the ferry transect were coincident with the tidal front reported previously by Loder and Greenberg (1986). Moreover, surface waters near the coast of Yarmouth, NS also are influenced by enhanced upwelling (Garrett & Loucks, 1975). Bisagni et al. (1996) observed enhanced chlorophyll *a* concentrations in the region of the tidal front off Nova Scotia, although their reported maximum concentrations were considerably lower than those we observed. Moreover, the high-chlorophyll *a* features seen at hydrographic fronts were generally associated with regions of lower vertical temperature gradients (<0.1 °C m^{-1}), but other factors clearly were involved in the formation of high chlorophyll patches beside vertical temperature gradients (Figs. 2–5, 6D) and mixed layer depth [compare chlorophyll concentrations (MMC Fig. 16–18) with mixed layer depth estimates (MMC Fig. 13–15)].

High acid-labile backscattering off Yarmouth was a persistent feature in the data set. There are two likely causes. There is a well-known calcite sediment deposit just off of Yarmouth (Manheim, 1972). The deposit, continuing to the north, is a large area of overstepped Tertiary sediments, mapped with seismic reflection profilers and surface grab samples. The rocks are buff to pink mudstones to siltstones, and they contain significant amounts of carbonate material (Pers. Comm. G. Fader, Bedford Inst. of Oceanography; August, 2002). The other possibility is that this water contained residual *E. huxleyi* blooms originating off the eastern coast of Nova Scotia. However, coccolith counts of samples from this SSW water (to be published separately) do not show elevated concentrations. Thus, resuspension of carbonate sediments in this well mixed water remains a more likely possibility.

4.2. Seasonal variability

Seasonal variability in Gulf of Maine SST and salinity was particularly obvious when cruise statistics were calculated. Based on the standard errors of the individual cruise means, SST and salinity varied substantially through the season, while density did not vary markedly (Figs. 2–5, 7). However, when cruise averages were examined, there were clear increases in salinity, density and chlorophyll as the season progressed (Fig. 18B–D). Spring and fall peaks in chlorophyll were also observed by Bisagni et al. (1996), both inshore and offshore based on measurements along the same cruise track. The individual cruise standard errors for SST, salinity, density and chlorophyll *a* were far smaller than the cruise-to-cruise variability. That is, the Gulf of Maine was responding to physical forcing at spatial scales of ~300 km over time scales as small as a few days (Fig. 18). This was likely related to wind-induced mixing, rather than due to horizontal advection. Care must be taken in this attribution, since our trips on the ferry were usually on days with winds out of the NW (which bring clear skies to the region) and the magnitude of the NW wind varied from light to gale force.

Monthly average *T*–*S* curves (Fig. 7) from June through September were consistent with the CCW flow of SSW (around JBW with its consistent density minimum), which then feeds into the EMCC, the offshore extension of which crosses the ferry track with a salinity similar to SSW but with temperature ~2 °C warmer. Minimum salinities were seen in June and September in the WMCC, presumably associated with riverine input of fresh water. By October, however, the *T*–*S* diagram virtually became a straight line, varying only in salinity, with WMCC and coastal waters off Yarmouth having lowest density and the JBW/SSW frontal boundary having highest density; this suggests that the JBW/SSW frontal boundary is an important source of upwelling in the region.

Changes in the relative importance of MBW and MIW were consistent with previous observations of Ramp et al. (1985), which showed significant changes in the volume of warm slope water present in the GOM over time scales of a few weeks (Fig. 8). While our observations were restricted to spring summer

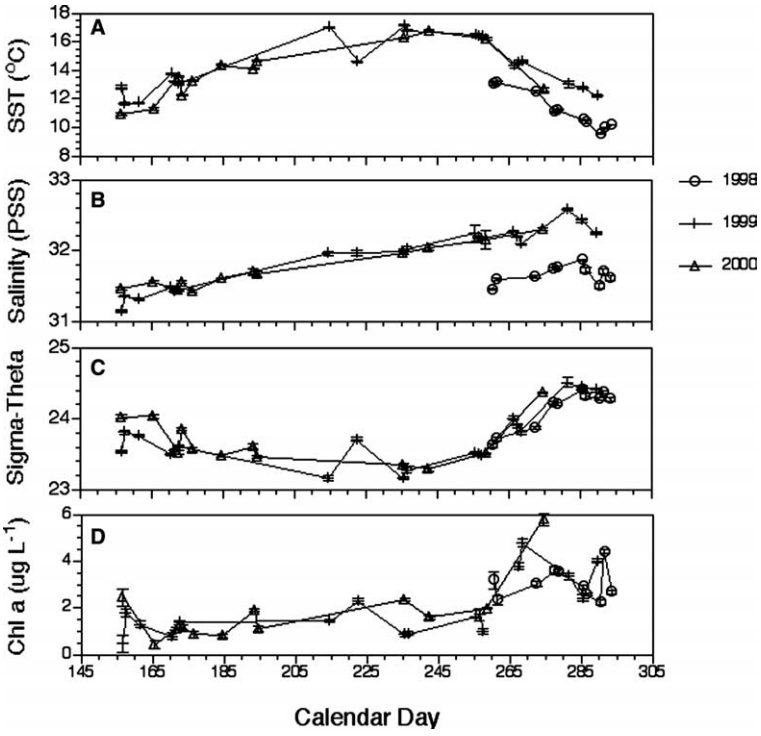

Fig. 18. Cruise-wide averages of SST, salinity, density, and chlorophyll *a* versus calendar day. Error bars represent one standard error. Data symbol key given beside panel B.

and fall, it was apparent that strong inflows of MBW were not confined just to winter months. When the proportion of MBW was increasing, warm, deep, water was observed on the NE side of the Northeast Channel (Fig. 8F–I), consistent with N. Atlantic slope water, which flows towards the west, being displaced northwards due to geostrophy, also in agreement with Ramp et al. (1985).

4.3. Long-term variability of hydrography and chlorophyll

Using the pooled data east of 69.6°W, we have compared 1999 and 2000 (the 1998 data set was too short to include). SST, salinity and density were significantly lower during 2000 than 1999, yet there was no significant change in the mean chlorophyll *a* between the two years (Fig. 19). We infer that a Gulf-wide decrease in SST of −0.25 °C and salinity of −0.2 PSS (which resulted in a Gulf-wide density decrease of ~0.1 sigma-theta unit from 1999 to 2000), was not enough to induce a significant change in the average chlorophyll *a* concentration in 2000. That is, phytoplankton biomass remained unchanged when one might have expected changes in physical mixing relative to the phytoplankton critical depth (Sverdrup, 1953). Lack of change in chlorophyll *a* also might have been due to other processes acting on the phytoplankton (i.e., biological factors such as grazing), which are of import in the control of phytoplankton biomass (Landry, 1993). Grazers would likely be affected by hydrographic variability at annual time scales and spatial scales of 300 km.

Within any one cruise, correlations of chlorophyll *a* and temperature were often not significant or only marginally so. However, pooling the entire three-year data set showed a highly significant, decreasing mean trend with a factor of ~2.7*X decrease* in chlorophyll *a* associated with a 10 °C increase in SST (chl

$a = 8.2616 * 0.904^{SST}$; $r^2 = 0.554$; SE of base = ±0.011; SE constant = ±0.171; total number of data points = 6462; number temperature bins = 60; $P < 0.001$; Fig. 20). Such a decrease in chlorophyll *a* associated with increasing temperature is inconsistent with the expected increases in algal physiological growth rates as a function of temperature (which usually have a Q_{10} of 2.1–2.3 Eppley, 1972).This could result from a whole suite of opposing processes such as: increased stratification and a slowing of upward diffusion of new nutrients (hence less new primary production; Balch, Bowler, & Byrne, 1997; Eppley & Peterson, 1979; Eppley & Renger, 1986), changes in phytoplankton species composition from cold-water algal species to warm-water species, changes in algal sinking rates (Smayda, 1970), temperature-dependent grazing rates, or changes in the species composition of grazers. The results in Fig. 20 are useful given the complexities of modeling ecosystem response to climate change; they demonstrate that, despite numerous (often opposing) influences of temperature on chlorophyll concentration due to biological, chemical and physical processes, broad changes in SST could have a significant, predictable effect on phytoplankton biomass in temperate waters.

Average algal pigment did not change significantly between 1999 and 2000, but the optical properties clearly did. Cruise-wide means for 514 nm b_{bpg}, b'_{bpg}, and b'_{bpg}/b_{bpg} showed significant seasonal and/or annual changes from 1999 to 2000 (Figs. 21 and 22). Backscattering probability at 514 nm showed significant seasonal variability (Fig. 21D), but no significant, annual change between 1999 and 2000 (Fig. 22). Comparison of Fig. 21A and B demonstrates that much (but not all) of the seasonal variability in total backscattering at 514 nm could be attributed to acid-labile scattering (from PIC). That is, increases in $b_{bp\,tot}$ were usually synchronous with commensurate peaks in b'_{bpg}. Honjo, Dymond, Prell, and Ittekkot (1999) suggested a conceptual biogeochemical model in which the background "carbonate ocean" of the Arabian Sea, dominated by calcifiers, evolved to a "silica ocean" in upwelling situations (such as in cyclonic eddies). Optical data for the Arabian Sea (Balch et al., 2001) supported the suggestion by Honjo et al. (1999) since

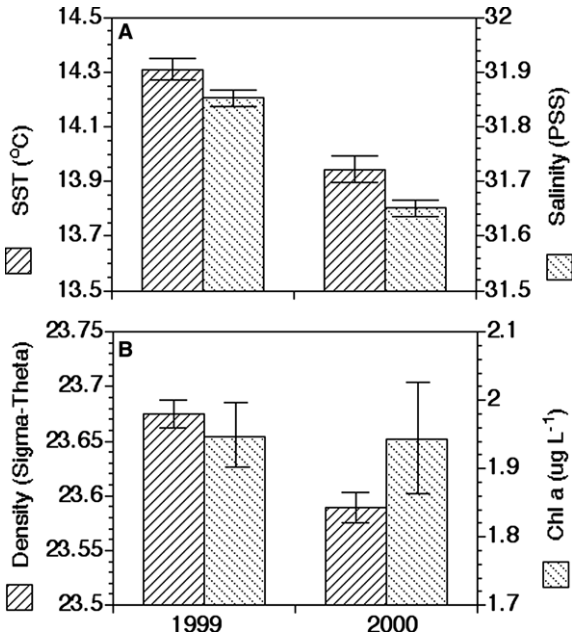

Fig. 19. Annual averages in SST, salinity, density and chlorophyll *a* for 1999 and 2000. Error bars represent one standard error about the mean. Key for each bar given on the respective *Y* axes.

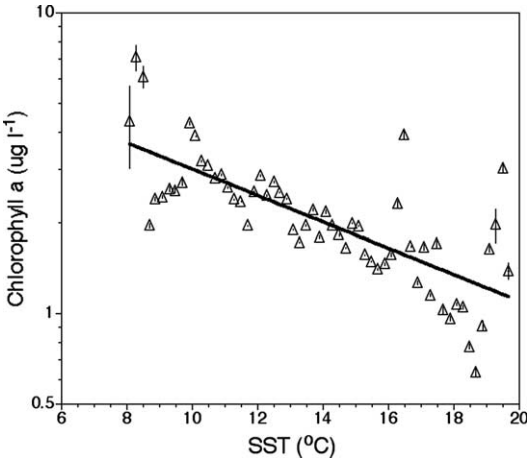

Fig. 20. Surface chlorophyll *a* versus SST in the Gulf of Maine for three years of ferry surveys. Data for this figure were binned and averaged every 0.1 °C in order to simplify the data presentation. Error bars represent ±one standard error in chlorophyll concentration for each temperature bin, which in most cases are smaller than the data symbols. Heavy black line shows least squares fit to the three years of data (chl $a = 8.2616 * \exp(-0.100858)$; $r^2 = 0.554$; total $n = 6462$).

much of the region's optical backscattering was dominated by calcite; regions of high $b_{\mathrm{bp\,tot}}$, such as the northern Arabian Sea and R'As al Hadd Front, also had high $b'_{\mathrm{b\,pg}}$.

In the Gulf of Maine, there was a constant background of calcite backscattering, but seasonal variability in backscattering was not influenced just by the appearance of diatoms, as suggested by Honjo; coccolithophore blooms also caused major perturbations to the optical backscattering. That is, mean $b_{\mathrm{bp\,tot}}$ at 514 nm of 0.003 m^{-1} showed spatial and temporal changes that were driven by the appearance of PIC in surface waters (e.g., Fig. 21; also compare the plot of total particulate backscattering MMC Fig. 21 line F) with its comparable acid-labile backscattering (MMC Fig. 24 line F). This does *not* mean that other scattering components, such as particulate detritus from rivers, were unimportant in modulating the $b_{\mathrm{bp\,tot}}$. At 412 nm, river-born particulate debris likely added to the b_{pg} in the WMCC and offshore extension of the EMCC (Figs. 3C, 4C and G, 13A). However, in general, coccolithophores (as well as diatoms) appeared to be important modulators of particulate backscattering of green light across the Gulf of Maine, and particularly in Jordan Basin.

4.4. CDOM and its seasonal patterns

The optical properties of CDOM and detritus also showed seasonality; mean $a_{\mathrm{pg\,412}}$ showed similar trends during of 1999 and 2000, with values gradually increasing through the summer season to a peak around day 280 (Fig. 23). The only exception was for day 165 of 2000, when $a_{\mathrm{pg\,412}}$ increased dramatically and the slope of the absorption between 412 and 440 nm (S) steepened dramatically (Fig. 23). The most obvious explanation for this short-term change in 412 nm absorption was that spring rains washed a pulse of concentrated CDOM into the Gulf of Maine.

Individual cruise means of $a_{\mathrm{pg\,412}}$ showed a fall peak in all three years (Fig. 23; MMC Figs. 35–37). Strikingly, the slope of the absorption values from 412 to 440 nm in the Gulf of Maine was usually −0.005 to −0.01, implying that dissolved organic matter was only weakly colored, and more representative of detritus and humic acid dominance than fulvic acid dominance (Roesler & Perry, 1989). In some marine environments, slopes of −0.015 to −0.020 have been observed (Mobley, 1994; Roesler & Perry, 1989). Even $b_{\mathrm{pg\,412}}$ showed significant increases in late summer/early fall, presumably due to increased dissolved and particu-

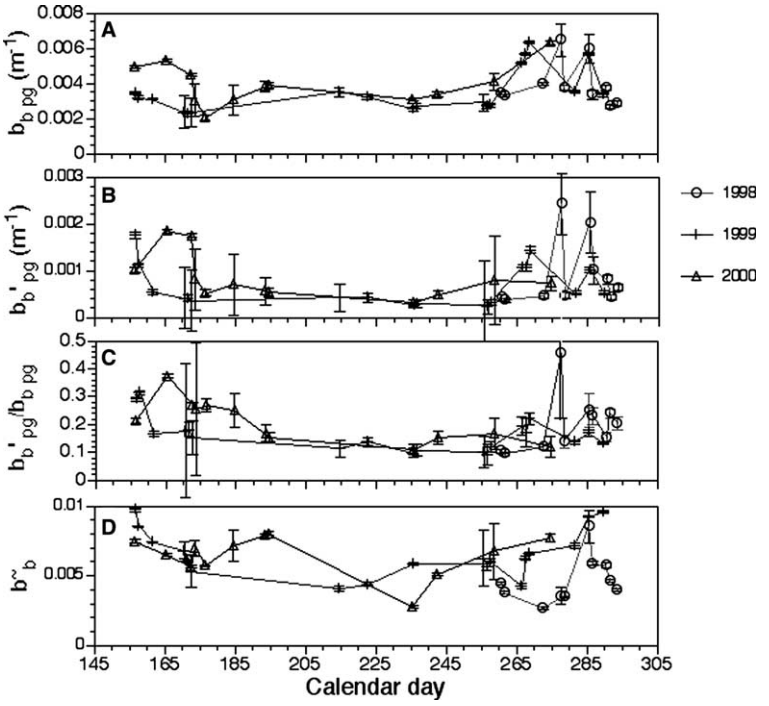

Fig. 21. Cruise-wide averages of $b_{b\,pg\,514}$, $b'_{b\,pg\,514}$, $b'_{b\,pg\,514}/b_{b\,pg514}$, and $b\tilde{}_{b\,514}$ vs calendar day. Data symbol key given to the right of panel B. Error bars represent standard errors about the mean.

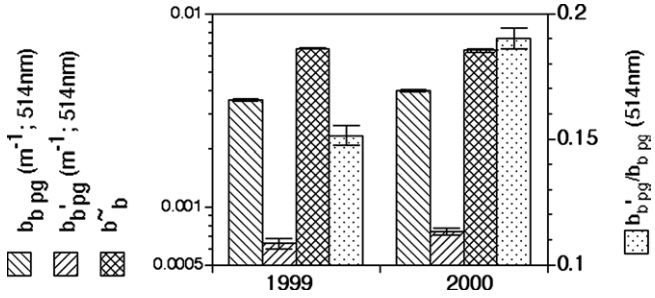

Fig. 22. Annual averages of $b_{b\,pg\,514}$, $b'_{b\,pg\,514}$, $b'_{b\,pg\,514}/b_{b\,pg\,514}$, and $b\tilde{}_{b\,514}$ for 1999 and 2000. Error bars represent standard errors about the mean. The key for the designation of each bar is given on the appropriate Y axes.

late detritus loads following fall rains (Fig. 5C, 23; MMC Fig. 30 lines I–K). One can hypothesize that if higher dissolved and suspended particulate loads come from rivers that empty into the Gulf of Maine, then $a_{pg\,412}$ would have increased in only the western part of the Gulf given the CCW circulation pattern. An alternate hypothesis is that increased discharge of CDOM-rich water from the Gulf of St. Lawrence likely would affect $a_{pg\,412}$ on *both* sides of Gulf of Maine, since it enters as SSW, then feeds into the Maine coastal current.

At variance with the above hypotheses (that fresh, riverine water and its associated CDOM were controlling $a_{pg\,412}$), is the observation that the fall peaks in $a_{pg\,412}$ were not associated with decreases in salinity, which one might have expected if there were greater river runoff during this time. In fact, salinity typically reached maximal values in the fall (Fig. 18). Another explanation for the fall peaks in

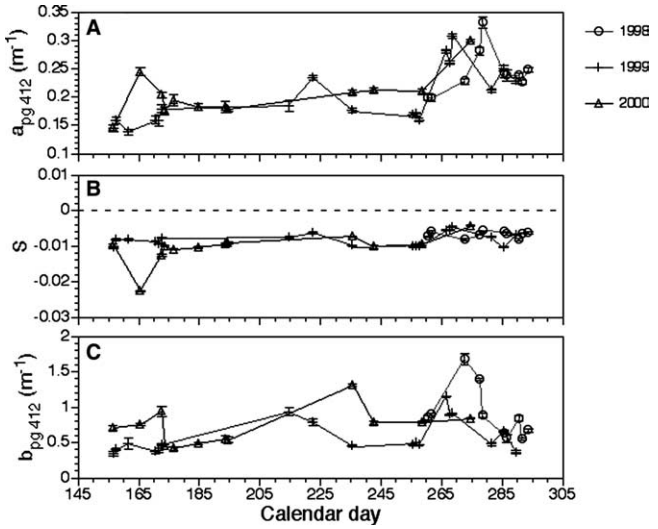

Fig. 23. Cruise-wide averages of a_{pg412}, S and b_{pg412} vs calendar day. Data symbol key is on right of panel A. Error bars represent standard errors about the mean.

a_{pg412} and b_{pg412} is that they resulted from upward mixing of a subsurface chlorophyll peak (with its associated algal-derived CDOM and particulate debris) as winds increased. Timing of the peaks in a_{pg412} and b_{pg412} was not simultaneous. Peaks in b_{pg412} in 1999 and 2000 preceeded the peaks in a_{pg412} by several days. This might have resulted from a bloom, followed by release of CDOM from the phytoplankton as it decayed.

CDOM and detritus optical signals changed significantly in the Gulf of Maine over time scales as short as 24 h, especially in the positions of sharp frontal boundaries (e.g., compare MMC Fig. 36 traces J,K and L, done on days 255–257 of 1999) and in the appearance/disappearance of peaks (e.g., compare MMC Fig. 36 traces M and N, done on days 267 and 268 of 1999, respectively). Short-term changes could have been caused by horizontal advection (requiring mean sustained current velocities up to ~28 cm s^{-1}, which is plausible given historical geostrophic estimates of the EMCC; Brooks & Townsend, 1989). Alternatively, the changes could have been caused by (a) vertical overturn of CDOM-rich/CDOM-poor waters or fast release of CDOM following a phytoplankton bloom event. Photo-oxidation of dissolved organic matter, combined with microbial respiration of the modified DOM, also could have caused rapid changes in CDOM absorption in the highly-illuminated surface waters (Andrews, Caron, & Zafiriou, 2000; Kieber, McDaniel, & Mopper, 1989; Kieber, Zhou, & Mopper, 1990; Mopper et al., 1991; Sikorski & Zika, 1993; Whitehead et al., 2000).

4.5. Long-term stability of CDOM distributions

Even with the rapid changes in CDOM absorption noted above, there were consistencies noted over entire seasons that suggest relative constancy in the processes controlling CDOM distribution. This is most obvious at the frontal boundaries on either side of Jordan Basin where spectral slopes of CDOM consistently had the least negative slopes, or in the WMCC where the most negative slopes were observed (MMC Fig. 39). When we sampled on consecutive days (e.g., September 12–14, 1999), we were able to make seawater optical measurements all the way into Portland Harbor. During those cruises, the reproducible, highly negative, spectral slopes of the WMCC water were readily apparent (MMC Fig. 39, traces J and K). Roesler and Perry (1989) described gelbstoff-dominated waters as having the most negative spectral

slopes in the blue end of the spectrum, while those dominated by detrital absorption (such as oligotrophic open ocean waters; HÆjerslev, 1980) have less negative slopes. This is entirely consistent with our observations in the WMCC and offshore extension of the EMCC. The more negative values in Jordan Basin also would suggest a strong influence of gelbstoff in this more stably stratified water mass, perhaps periodically supplied by the extensions of EMCC water (Pettigrew et al., 1998). Indeed, Bisagni et al. (1996) described evidence for Maine Coastal Current water being advected offshore; they found an estuarine zooplankton species in offshore waters, implying horizontal advection from the coastal regions. The source of the CDOM often-observed in the well-mixed SSW off of Nova Scotia (Figs. 2H, 3D and H; MMC Figs. 35–40) was probably water advected from the Gulf of St. Lawrence estuary, transported south along the east coast of Nova Scotia, then swept into the SSW off of Yarmouth (Smith, 1983; Sutcliffe et al., 1976). This is especially likely given that these waters had a well-defined salinity decrease (Figs. 2A, 3A and E: MMC Figs. 4–6).

4.6. Deep mixing of detritus/CDOM

We hypothesize that the less steep spectral absorption slopes observed at the frontal boundary waters on either side of Jordan Basin were indicative of vertical mixing, which brought deeper water, with more detritus and less gelbstoff (from deeper chlorophyll maximum populations), to the surface. If this is true, then the spectral slope of blue absorption should have uniformly decreased across the transect after major storm events. This, indeed, was apparent after the passage of hurricanes Floyd (which passed through the Gulf of Maine on 17 September, 1999) and Gert (which tracked east of Nova Scotia on 23 September, 1999). The storms dropped ~19 cm of rain within a 1 week (as measured by the National Weather Service in Portland, ME; data not shown). Stream flow in the Penobscot River increased by a factor of 8 during this same period (USGS; data not shown). Even with the increased runoff, there was not a pronounced salinity decrease in the surface Gulf of Maine following the passage of the two storms (MMC Fig. 5; compare traces M and N). In fact, surface water densities actually *increased* after the storms (MMC Fig. 8; compare traces M and N), suggesting that the major effect of the storm was to cause vertical overturn of the water column between our trips of 14 and 24 September, 1999. (Note, we also sampled on 23 September, 1999, but the heavy seas from hurricane Gert broke our outboard water-sampling pipe. We were unable to collect any continuous underway data after the break, only bucket samples and XBT profiles). The extent of the storm-induced vertical mixing that occurred between 23 and 24 September, 1999, was apparent in (a) decreases of the vertical temperature gradient over the top 50 m (compare MMC Fig. 11, traces N and O) and (b) increases in the mixed layer depth from ~4 to ~10 m over the 24-h period (compare MMC Fig. 14, traces N and O). The spectral slopes of blue absorption were considerably less steep across the Gulf of Maine *after* the mixing event (compare MMC Fig. 39, traces L and M), consistent with our above hypothesis that detritus was mixed from deeper in the water column.

4.7. The Case II nature of the Gulf of Maine

Despite the temporal changes in CDOM absorption noted above, the overall Case II nature of the Gulf of Maine waters is striking. The difference between observed b_{550} and b_{550} predicted from the ambient chlorophyll *a,* showed that Gulf of Maine surface waters were Case II_{partic}, in all periods except the fall (Figs. 2–5, 17A; MMC Figs. 41–43). The seasonal pattern was even more obvious when considering individual cruise averages (Fig. 24A). Observed mean b_{550} was slightly less than expected in the spring (based on chlorophyll *a* alone), and considerably lower in the fall (by ~0.5–0.7 m^{-1}). This occurred when mixed layers were deeper, and surface optical properties were influenced by deeper phytoplankton populations from the chlorophyll maximum (in which the optical properties were driven by phytoplankton, not other

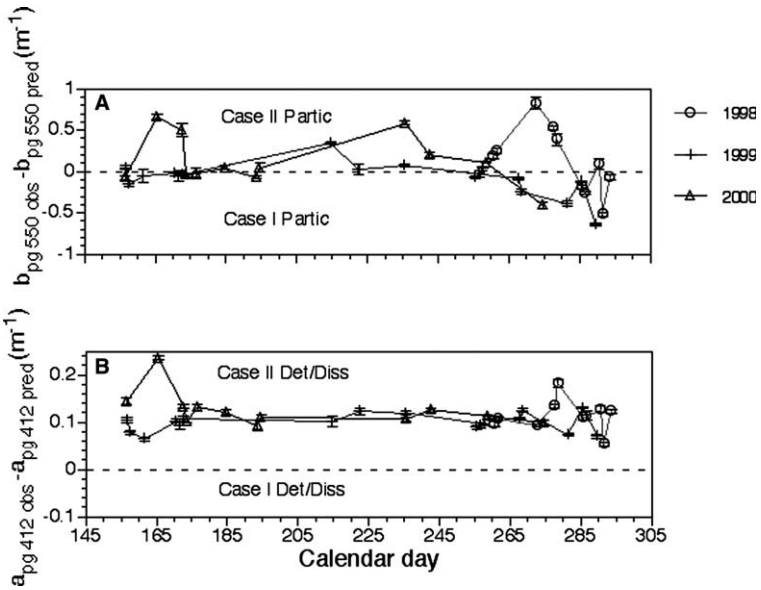

Fig. 24. Annual averages of Case II_{partic} and Case II_{diss} indices. Data symbol key given to right of panel A. Negative values indicate Case I conditions. Positive values of either axis designate Case II conditions for particles or dissolved plus detrital material, respectively. Error bars represent standard errors about the mean.

sedimentary or dissolved material). During the summer months, however, individual cruise mean b_{550} was greater than expected based on ambient chlorophyll, indicative of water that was Case II_{partic}.

The coccolithophore bloom of 2000 clearly caused the Case II_{partic} peak seen at day 165 (Fig. 24; MMC Fig. 43 line B). Technically, these should be considered anomalous Case I conditions, since the highly-scattering particles consisted of living algal cells and their associated debris (including coccoliths) (Gordon & Morel, 1983), as opposed to non-algal particles. While there can be ambiguities in the definition of Case II waters during relatively rare coccolithophore blooms, such blooms are usually exceptions to the more varied phytoplankton assemblages found in the Gulf of Maine; the equations used here to define the presence of Case II conditions are still robust.

The cause of the high Case II_{partic} values across much of the transect on day 272, 1998 (Fig. 24; MMC Fig. 41 line C) is not known. There was no observable relation of the Case II_{partic} values to the temperature, salinity and density data for that day (see line C in MMC Figs. 1, 4, 7). Nonetheless, there was a significantly lower salinity during that season, indicating more river influence (Fig. 18B). High annual average Case II_{partic} values were also observed off the Nova Scotia coast in 1998 (Fig. 17A; MMC Fig. 41 F–J), suggesting an origin of the high concentrations of suspended particles outside the Gulf of Maine, perhaps the St. Lawrence estuary as described above.

While Gulf of Maine waters were Case II_{partic} part of the time, they were Case II_{diss} virtually all the time (Figs. 2–5, 17B; MMC Figs. 44–46). This was even more obvious when individual cruise mean values were calculated (Fig. 24B); a_{pg412} was virtually always $\sim$0.1 m^{-1} greater than predicted by the Morel (1991) equations. Lowest a_{pg412} values were seen in spring and fall, as was observed for the Case II_{partic} waters.

One interesting anomalous peak in Case II_{diss} index was seen on day 165 during the spring of 2000 (Fig. 24B; MMC Fig. 46 line B), the period of the above-mentioned coccolithophore bloom. There was no indication from the raw or averaged salinity data (MMC Fig. 6 line B; Fig. 18) why there should have been elevated Case II_{diss} values on this day, but the mean cruise a_{pg412} was, clearly, significantly greater than the surrounding sample dates (Fig. 23A). It should *not* have resulted from light absorption of calcite cocc-

oliths as they absorb minimal light at 412 nm (Balch, Holligan, Ackleson, & Voss, 1991). Nonetheless, it is known that the calcite matrix can absorb appreciable amounts of dissolved organic matter (Troy, Li, & MacKenzie, 1997). Thus, we cannot eliminate the hypothesis that the high $a_{pg\,412}$ resulted from CDOM bound to suspended coccoliths of a coccolithophore bloom. Alternative hypotheses should be considered for the peak in $a_{pg\,412}$ values. Advective input of river-borne CDOM and detritus, presumably would have been accompanied by a simultaneous salinity minimum. This was not observed. Vertical supply of nonphotooxidized CDOM from below, on the other hand, likely would have been associated with a salinity *increase,* which indeed was observed, albeit a small one (Fig. 18).

There are other associations between mixing and $a_{pg\,412}$ that indicate that these dissolved Case II waters constitute a large part of the euphotic layer. In the fall of 1998, deepening mixing (MMC Fig. 13; traces D-F) was associated with declining $a_{pg\,412}$ values in the WMCC up until day 287 (Fig. 24B; MMC Fig. 35 lines E–H), implying a lesser relative influence of CDOM in the deeper waters. As with the major hurricane mixing events noted on 23 September 1998, the spectral slope of the blue absorption became less steep after such increases in mixed layer depth (compare gulf-wide changes in the spectral slope for 1998 cruises; MMC Fig. 38, curve C onwards). Nonetheless, the fact that the surface waters still showed strong Case II_{diss} properties (MMC Fig. 46) suggests that these waters extended to typical mixed layer depths of 10–30 m.

4.8. Origin of Case II waters outside or inside the Gulf of Maine?

While the Gulf of Maine was Case II_{partic} in 2000, but not 1999 (see Fig. 25B, noting the reduced scales on the *Y*-axis compared to Fig. 17A), even in 1999, waters were on average within 0.08 m^{-1} of being Case II_{partic}. The overriding question is the source of these particles in waters as far as 150 km from their coastal riverine source. One possibility is that particles resuspended via intense tidal mixing in the Bay of Fundy were swept offshore in the extension of the EMCC. This interpretation is well supported by SeaWiFS

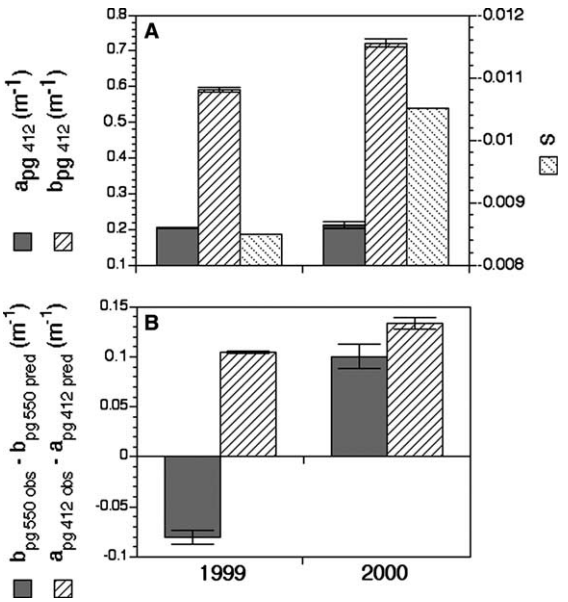

Fig. 25. Annual averages of $a_{pg\,412}$, $b_{pg\,412}$, *S*, Case II_{partic} and Case II_{diss} index. Error bars represent standard errors about the mean. Color-coding of bars of the histograms is given on the corresponding *Y*-axis.

and AVHRR imagery which shows how filaments of coastal water can reach clear across the Gulf of Maine to the northern flank of Georges Bank and Browns Bank (see example in Fig. 26). The offshore extension of the EMCC is known to be important in the spatial distribution of nutrients and dinoflagellates that are found offshore (Pettigrew et al., 1998; Townsend, Pettigrew, & Thomas, 2001).

If the above hypothesis were true, then there should have been a large increase in the Case II_{partic} index going from the SSW to EMCC and WMCC waters. This is because SSW water, flowing CCW around the Gulf of Maine, presumably would have received a large particle load due to the tidal mixing in the Bay of

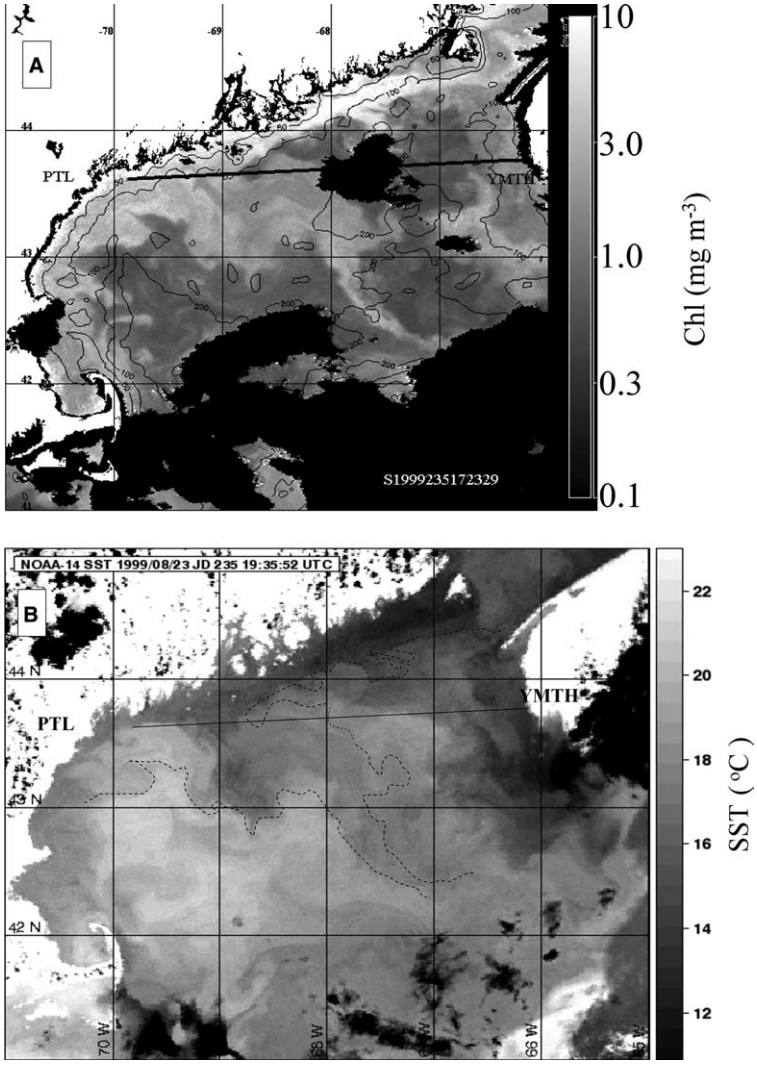

Fig. 26. (A) SeaWiFS image from the Gulf of Maine, 23 August, 1999, showing filament of high chlorophyll water extending across the Gulf to the northeast filament of Georges Bank (in this image obscured by cloud). The gray-scale color bar is shown to the right of the image. Black areas show cloud distribution. Bathymetry contours have been superimposed on this image. The ferry transect is shown between Yarmouth ("Ymth") and Portland ("PTL"). (b) NOAA-14 AVHRR SST image from same day as above SeaWiFS image. An outline of the filament shown in panel A has been placed over the SST image for reference. It can be seen that the southern border of the filament corresponds to an obvious thermal front.

Fundy, before the waters passed into the EMCC and WMCC. No such clear increase in the Case II_{partic} index was evident, however. Moreover, the fact that some of the highest Case II_{partic} values were seen in buoyant, low salinity waters off of Yarmouth, suggests that Gulf of St. Lawrence waters could have mixed with SSW and been a significant source of the particles to the Gulf of Maine. An alternative hypothesis is that, since the surface waters of the Gulf of Maine are overwhelmingly Case II_{diss} (Figs. 17 and 24), then many of the particles might be polymer-gel-like aggregates formed *in situ* from CDOM (Chin et al., 1998). If this were the case, then there should be some correlation between the Case II_{diss} and Case II_{partic} indices. Indeed, there is a low but significant correlation between these two indices (Fig. 27). The reader will note that for those years were high values of the Case II_{partic} index were seen off of Yarmouth, so were high values of the Case II_{diss} index (Fig. 17). Thus, demonstrating the source of the particles that contribute to the Case II_{partic} nature of the Gulf of Maine is complex. Obviously, short-term changes in the Case II_{partic} index (days to months) are more likely to be due to particle production and resuspension events within the Gulf, while longer (e.g., annual or greater) time-scale changes could be due to changes in particle supply from outside the Gulf. This issue will be addressed further in a subsequent communication.

4.9. The volume scattering function in the Gulf of Maine

One of the more striking results from this study was the significant deviation of the volume scattering functions from the standard shape of the coastal volume scattering function of Petzold (1972). The Petzold coastal phase function is commonly used in radiative transfer models (Mobley, 1999). Substituting normalized values of β_{45} and β_{135} that are 70–80% and 125–150%, respectively, of the Petzold model (Figs. 15 and 16), will have large consequences in radiative transfer calculations, as the forward scattered light is diminished and backscattered light is enhanced. It is noteworthy that the error bars on the Gulf of Maine data only rarely included the Petzold values. These deviations are not surprising given that Petzold's data for the coastal VSFs came from just one location, San Pedro Channel, California, over a time scale of days, as compared to our 315 km transect run over 3 years. We suggest that future optical calculations requiring estimates of the VSF, be revised to values given in Table 2, which cover a wide range of meso- and eutrophic regions.

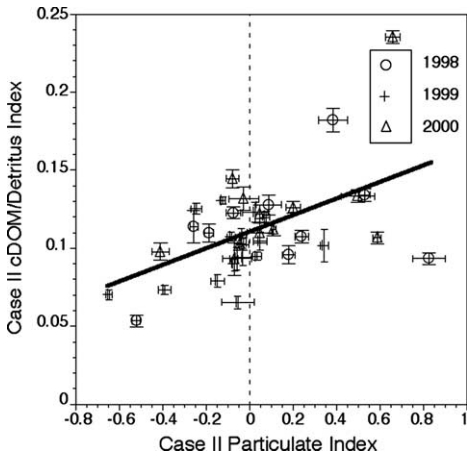

Fig. 27. Cruise-wide averages of Case II_{diss} index vs Case II_{partic} index for three years of ferry data. Error bars represent standard errors about the mean. Least-squares fit to data is shown with the black line ($Y = 5.31 \times 10 - 2X + 0.109$; $r^2 = 0.277$; $n = 39$; $P < 0.01$). Data symbol key given on upper right of figure.

Equally striking was the observed seasonal variability in β_{45} (lower values in spring and fall and greatest values in the summer) which, to our knowledge, has not been observed before. Such a change would likely result from community shifts in the phytoplankton community (data to be shown elsewhere) related to changes in the shape, size, and refractive index of the particles. The relative variability in forward angle volume scattering due to these community shifts was 10–30% (Fig. 15A). While the β_{135} values did not show the same steady shift with seasons as β_{45}, one can see some effects of coccolithophores on β_{135}, such as during the 2000 *E. huxleyi* bloom (days 165–193), when large normalized β_{135} values were observed with large standard deviations (Fig. 15B). Since small particles contribute more of the scattering at large angles, shifts to greater β_{135} values may reflect a steepening of the particle size distribution function (i.e., more small particles relative to the larger, rarer, particles). Given the variability in volume scattering that can be attributed to seasonal (Fig. 15) and spatial effects (Fig. 16), future models of light scattering in the sea will require better parameterization of these changes in VSF shape as a function of taxonomy.

5. Conclusions

We conclude that surface optical properties were strongly coupled with hydrographic variability in the Gulf of Maine. Elevated concentrations of phytoplankton, detrital particles and CDOM were associated with hydrographic frontal boundaries, which, in turn, caused significant variability in spectral absorption and scattering. Gulf-wide averages of hydrographic properties demonstrated that the volume of Maine Surface Water present in the Gulf of Maine is correlated to the mean surface density across the region, as well as to mean surface chlorophyll *a* concentrations. Significant variability in the particle scattering of Case I waters was associated with growth of marine algae at frontal boundaries, particularly coccolithophores, which dominated particulate backscattering during a bloom in 2000. The surface Gulf of Maine was Case II_{partic} about half the time and Case II_{diss} virtually all of the time. The usual source of the Case II_{diss} water was likely rivers, given that 412 nm scattering and absorption were greatest in low salinity waters of the WMCC. However, during specific fall mixing events, significant increases in 412 nm absorption and backscattering were associated with the upward mixing of higher salinity water. This water likely contained phytoplankton and algal-associated detritus/CDOM from the chlorophyll maximum; hence it was more accurately Case I in character. The Case II_{partic} index was only moderately correlated with the Case II_{diss} index. Case II_{partic} water in the Gulf of Maine may have several sources: (a) river-borne suspended matter from Maine coastal waters, (b) intrusions of buoyant Gulf of St. Lawrence water that flows into the Gulf of Maine as part of the SSW or (c) macro-aggregates formed from the annealing of polymer microgels from dissolved organic material. Particle VSFs from the Gulf of Maine were significantly different from those described by Petzold (1972) for coastal waters, and there were significant spatial and temporal changes in VSF shape. A highly significant, inverse trend was observed between mean surface chlorophyll biomass and mean SST. This trend, which integrated many different physical, ecological and physiological phenomena, provides a means to predict the effect of a long-term temperature changes on the phytoplankton biomass of the Gulf of Maine.

Acknowledgements

This Gulf of Maine time series work could not have been done without the tremendous support of the owners, captains, crew and staff of the *M/S Scotia Prince* (Scotia Prince Cruises, formerly Prince of Fundy, LTD). We are deeply indebted to them for the opportunity to use the ferry as a sampling platform; their untiring, "can-do" attitude is a real credit to their business. Thanks also go to Rob McCabe, Ben Allen and Ned Forrester (Woods Hole Oceanographic Institution, Ocean Systems Laboratory) for help in building

our mobile sampling laboratory. Chris Conary and Matt Wilder (Sheepscot Machine Company, Edgecomb, ME) helped fabricate many items used for water sampling. We also thank several anonymous reviewers for comments on earlier drafts of this manuscript. This work was generously supported, wholly or in part, by various grants from NASA (NAS5-97268; NAS5-31363; NAG5-10622; NNG04Gl11G; NNG04HZ25C; NASA EPSCOR EP-02-14), NOAA (40-AA-NE-005996), NSF (OCE-0136541; OCE-0325937) and ONR (N00014-98-1-0882; N00014-01-1-0042) to WMB and NASA grant no. NAG5-11219 to JIG.

Appendix A. Supplementary data

Supplementary data associated with this article can be found, in the online version, at doi:10.1016/j.pocean.2004.09.003.

References

Aiken, J., Rees, N., Hooker, S., Holligan, P., Bale, A., Robins, D., Moore, G., Harris, R., & Pilgrim, D. (2000). The Atlantic meridional transect: Overview and synthesis of data. *Progress in Oceanography, 45*, 257–312.

Andrews, S. S., Caron, S., & Zafiriou, O. C. (2000). Photochemical oxygen consumption in marine waters: A major sink for colored dissolved organic matter. *Limnology and Oceanography, 45*(2), 267–277.

Balch, W. M. (2004). Re-evaluation of the physiological ecology of coccolithophores. In H. R. Thierstein & J. R. Young (Eds.), *Coccolithophores – From molecular processes to global impact* (pp. 165–190). New York: Springer-Verlag.

Balch, W. M., Bowler, B., & Byrne, C. F. (1997). Sea surface temperature gradients, baroclinicity, and vegetation gradients in the sea. *Journal of Plankton Research, 19*, 1829–1858.

Balch, W. M., Drapeau, D., & Fritz, J. (2000). Monsoonal forcing of calcification in the Arabian Sea. *Deep-Sea Research II, 47*, 1301–1337.

Balch, W. M., Drapeau, D., Fritz, J., Bowler, B., & Nolan, J. (2001). Optical backscattering in the Arabian Sea-continuous underway measurements of particulate inorganic and organic carbon. *Deep Sea Research I, 48*, 2423–2452.

Balch, W. M., & Drapeau, D. T. (2004). Backscattering by coccolithophorids and coccoliths: Sample preparation, measurement and analysis protocols. In J. L. Mueller, G. S. Fargion, & C. R. McClain (Eds.). *Ocean optics protocols for satellite ocean color sensor validation, Revision 5: biogeochemical and bio-optical measurements and data analysis protocols* (Vol. 5, pp. 27–36). Greenbelt, MD: National Aeronautical and Space administration, Goddard Space Flight Space Center.

Balch, W. M., Drapeau, D. T., Cucci, T. L., Vaillancourt, R. D., Kilpatrick, K. A., & Fritz, J. J. (1999). Optical backscattering by calcifying algae – Separating the contribution by particulate inorganic and organic carbon fractions. *Journal of Geophysical Research, 104*, 1541–1558.

Balch, W. M., Eppley, R. W., Abbott, M. R., & Reid, F. M. H. (1989). Bias in satellite-derived pigment measurements due to coccolithophores and dinoflagellates. *Journal of Plankton Research, 11*, 575–581.

Balch, W. M., Holligan, P. M., Ackleson, S. G., & Voss, K. J. (1991). Biological and optical properties of mesoscale coccolithophore blooms in the Gulf of Maine. *Limnology and Oceanography, 36*, 629–643.

Berner, R. A. (1976). The solubility of calcite and aragonite in seawater at atmospheriric pressure and 34.5 ppt salinity. *American Journal of Science, 276*(6), 713–730.

Bigelow, H. B. (1914). Explorations in the Gulf of Maine, July and august, 1912, by the United States Fisheries schooner Grampus. Oceanography and notes on the plankton. *Bulletin Museum of Comparative Zoology at Harvard College, 58*(2), 29–147.

Bigelow, H. B. (1926). *Plankton of the offshore waters of the Gulf of Maine (968)*. Washington DC: US Department of Commerce.

Bigelow, H. B. (1927). Physical oceanography of the Gulf of Maine. *Fisheries Bulletin, 40*, 511–1027.

Bisagni, J. J., Gifford, D. J., & Ruhsam, C. M. (1996). The spatial and temporal distribution of the Maine Coastal Current during 1982. *Continental Shelf Research*, 1–24.

Bogden, P. S. (2002). GoMOOS: Transition to an operational observing system. Paper presented at the Ocean Sciences Meeting, Honolulu, HI.

Boyd, C. M. (1985). Is secondary production in the Gulf of Maine limited by the availability of food? *Archiv fur hydrobiologie. Beihefte: Ergebnisse de limnologie, 21*, 57–65.

Brooks, D. (1985). Vernal circulation in th Gulf of Maine. *Journal of Geophysical Research, 90*(C3), 4687–4705.

Brooks, D. A. (1992, 8–10 Jan. 1991). A brief overview of the physical oceanography of the Gulf of Maine. Paper presented at the Gulf of Maine Scientific Workshop, Woods Hole, MA, USA.

Brooks, D. A., & Townsend, D. (1989). Variability of the coastal current and nutrient pathways in the Gulf of Maine. *Journal of Marine Research, 47*, 303–321.

Campbell, J. W., & O'Reilly, J. E. (1988). Role of satellites in estimating primary productivity on the northwest Atlantic continental shelf. *Cont. Shelf. Res., 8*, 179–204.

Chavez, F. P., Herlien, R., & Thurmond, G. (1994). OASIS – acquisition system for moorings/drifters. *Sea Technology, 35*(2), 51–59.

Chin, W. C., Orellana, M. V., & Verdugo, P. (1998). Spontaneous assembly of marine dissolved organic matter into polymer gels. *Nature, 391*, 568–572.

Christensen, J. P., Townsend, D. W., & Montoya, J. P. (1995). Water column nutrients and sedimentary denitrification in the Gulf of Maine. *Continental Shelf Research, 16*, 489–515.

Davenport, R., Neuer, S., Hernandez-Guerra, A., Rueda, M. J., Llinas, O., Fischer, G., & Wefer, G. (1999). Seasonal and interannual pigment concentration in the Canary Islands region from CZCS data and comparison with observations from the ESTOC. *International Journal of Remote Sensing, 20*(7), 1419–1433.

Dickey, T., Zedler, S., Yu, X., Doney, S. C., Frye, D., Jannasch, H., Manov, D., Sigardson, D., McNeil, J. D., Dobeck, L., Gilboy, T., Bravo, C., Siegel, D. A., & Nelson, N. (2001). Physical and biogeochemical variability from hours to years at the Bermuda testbed mooring site: June 1994–March 1998. *Deep-Sea Res II, 48*, 2105–2140.

Drinkwater, K. F., Mountain, D. B., & Herman, A. (1999). Variability in the slope water properteis off eastern North America and their effects on the adjacent shelves (1999/O:08): ICES C.M.

Eppley, R. W. (1972). Temperature and phytoplankton growth in the sea. *Fishery Bulletin, 70*, 1063–1085.

Eppley, R. W. (1986). *Plankton dynamics of the Southern California Bight* (15). New York: Springer-Verlag.

Eppley, R. W., & Peterson, B. (1979). Particulate organic matter flux and planktonic new production in the deep ocean. *Nature, 282*, 677–680.

Eppley, R. W., & Renger, E. H. (1986). Nitrate-based primary production in nutrient-depleted surface waters off California. *Océanographie Tropicale, 21*(2), 229–238.

Fargion, G., & McClain, C. R. (2000). Three years of ocean color instrument intercomparisons and cross-calibrations by the SIMBIOS project (1997–2000). *Proceedings of SPIE, 4172*, 44–55.

Fargion, G. S., & McClain, C. R. (2001). SIMBIOS project 2000 annual report. Greenbelt, MD: National Aeronautics and Space Administration, Goddard Space Flight Center.

Garrett, C. J. R., & Loucks, R. H. (1975). *Upwelling along the Yarmouth shore of Nova Scotia*, 116–117.

Gordon, H. R., & Morel, A. Y. (1983). *Remote assessment of ocean color for interpretation of satellite visible imagery – a review*. New York: Springer-Verlag.

Grassle, F., Petrecca, R., & von Alt, C. (1995). *Leo-15: A system for continuous long-term ecosystem investigations on the continental shelf*.

Højerslev, N. K. (1980). *On the origin of yellow substance in the marine environment, studies in physical oceanography* (Vol. 42, pp. 39–56). University of Copenhagen, Institute of Physical Oceanography.

Hansell, D. A., & Carlson, C. A. (2001). Marine dissolved organic matter and the carbon cycle. *Oceanography, 14*(4), 41–49.

Holligan, P. M., Balch, W. M., & Yentsch, C. M. (1984). The significance of subsurface chlorophyll, nitrite and ammonium maxima in relation to nitrogen for phytoplankton growth in stratified waters of the Gulf of Maine. *Journal of Marine Research, 42*, 1051–1073.

Honjo, S., Dymond, J., Prell, W., & Ittekkot, V. (1999). Monsoon-controlled export fluxes to the interior of the Arabian Sea. *Deep-Sea Research II, 46*, 1859–1902.

Hopkins, T. S., & Garfield, N. (1979). Gulf of Maine Intermediate Water. *Journal of Marine Research, 37*, 103–139.

JGOFS. 1996. Protocols for the Joint Global Ocean Flux Study (JGOFS) core measurements (Report no. 19 of the Joint Global Ocean Flux Study). Bergen, Norway: Scientific Committee on Oceanic Research, International Council of Scientific Unions, Intergovernmental Oceanographic Commission.

Joyce, T. M., & Robbins, P. (1996). The long-term hydrographic record at Bermuda. *Journal of Climate, 9*, 3121–3131.

Kieber, D. J., McDaniel, J., & Mopper, K. (1989). Photochemical source of biological substrates in sea water: Implications for carbon cycling. *Nature, 341*, 637–639.

Kieber, R. J., Zhou, X., & Mopper, K. (1990). Formation of carbonyl compounds from UV-induced photodegradation of humic substances in natural waters: Fate of riverine carbon in the sea. *Limnology and Oceanography, 35*(7), 1503–1515.

Koike, I., Hara, S., Terauchi, K., & Kogure, K. (1990). Role of sub-micrometer particles in the ocean. *Nature, 345*, 242–244.

Kuo, F. Y. (1991). Monthly mean time series of temperature and salinity in Monterey Bay, 1951–1991. Unpublished Masters, Naval Postgrad. Sch., Monterey, CA (USA).

Landry, M. R. (1993). Estimating rates of growth and grazing mortality of photoautotrophic plankton by dilution. In P. F. Demp, B. F. Sherr, E. B. Sherr, & J. J. Cole (Eds.), *Handbook of methods in aquatic microbial ecology* (pp. 715–722). Boca Raton, FL: Lewis Publishers.

Loder, J. W., & Greenberg, D. A. (1986). Predicted positions of tidal fronts in the Gulf of Maine region. *Continental Shelf Research, 1986*, 397–414.

Lynch, D. R., Holboke, M. J., & Naimie, C. E. (1997). The Maine coastal current: Spring climatological circulation. *Continental Shelf Research, 17*(6), 605–634.

Maffione, R. A., & Dana, D. R. (1997). Instruments and methods for measuring the backward-scattering coefficient of ocean waters. *Applied Optics, 36*(24), 6057–6067.

Manheim, F. T. (1972). Mineral resources off the northeastern coast of the United States (669). US Geological Survey, US Department of the Interior, Washington DC.

Mobley, C. D. (1992). The optical properties of water. In M. Bass (Ed.), *Handbook of Optics* (Second ed.). New York: McGraw-Hill Book Co.

Mobley, C. D. (1994). *Light and water: Radiative transfer in natural waters*. New York: Academic Press.

Mobley, C. D. (1999). *Hydrolight 4.0 Users' Guide*. Mercer Island, WA: Sequoia Scientific, Inc..

Mopper, K., Zhou, X., Kieber, R. J., Kieber, D. J., Sikorski, R. J., & Jones, R. D. (1991). Photochemical degradation of dissolved organic carbon and its impact on the oceanic carbon cycle. *Nature, 353*, 60–62.

Morel, A. (1980). In-water and remote measurement of ocean color. *Boundary Layer Meterology, 18*, 177–201.

Morel, A. (1991). Light and marine photosynthesis: A spectral model with geochemical and climatological implications. *Progress in Oceanography, 26*, 263–306.

Mountain, D. G., & Jessen, P. F. (1987). Bottom waters of the Gulf of Maine, 1978–1983. *Journal of Marine Research, 45*, 319–345.

O'Reilly, J. E., Maritorena, S., Mitchell, B. G., Siegel, D. A., Carder, K. L., Garver, S. A., Kahru, M., & McClain, C. (1998). Ocean color chlorophyll algorithms for SeaWiFS. *Journal of Geophysical Research, 103*(C11), 24937–24953.

Pegau, W. S., Gray, D., & Zaneveld, J. R. (1997). Absorption of visible and near-infrared light in water: The dependence on temperature and salinity. *Applied Optics, 36*(24), 6035–6046.

Pettigrew, N. R., Roesler, C., Beard, M. K., Bogden, P., Incze, L., Irish, J. D., Panchang, V., Perrie, W., Thomas, A., Townsend, D. W. & Xue, H. (2002). *Implementation of the Gulf of Maine Ocean Observing System (GoMOOS)*. Paper presented at the Ocean Sciences Meeting, Honolulu, HI, USA.

Pettigrew, N. R., Townsend, D. W., Xue, H., Wallinga, J. P., Brickley, P. J., & Hetland, R. D. (1998). Observations of the Eastern Maine Coastal Current and its offshore extensions in 1994. *Journal of Geophysical Research, 103*(C13), 623–630.

Petzold, T. J. (1972). Volume scattering functions for selected ocean waters (Tech.), Univ. Calif. Scripps Inst. Oceanogr.

Pingree, R. D., Pugh, P. R., Holligan, P. M., & Forster, G. R. (1975). Summer phytoplankton blooms and red tides along tidal fronts in the approaches to the English Channel. *Nature, 258*, 672–677.

Prieur, L., & Sathyendranath, S. (1981). An optical classification of coastal and oceanic waters based on the specific spectral absorption curves of phytoplankton pigments, dissolved organic matter, and other particulate materials. *Limnology and Oceanography, 26*(4), 671–689.

Ramp, S. R., Schlitz, R. J., & Wright, W. R. (1985). The deep flow through the Northeast Channel, Gulf of Maine. *Journal of Physical Oceanography, 15*, 1790–1808.

Reid, J. L. (1988). Physical oceanography, 1947–1987. *CalCOFI Rep., 29*, 42–65.

Roesler, C. S., & Perry, M. J. (1989). Modeling in situ phytoplankton absorption from total absorption spectra in productive inland marine waters. *Limnology and Oceanography, 34*(8), 1510–1523.

Sathiyamoorthy, S., & Moore, G. W. K. (2002). Buoyancy Flux at Ocean Weather Station Bravo. *Journal of Physical Oceanography, 32*(2), 458–474.

Schroeder, E., & Stommel, H. (1969). How representative is the series of Panulirus stations of monthly mean conditions off Bermuda?. *Progress in Oceanography, 5*, 31–40.

Siegel, D. A., Karl, D. M., & Michaels, A. F. (2001). Interpretations of biogeochemical processes from the US JGOFS Bermuda and Hawaii time-series sites. *Deep-Sea Research II, 48*(8–9), 1403–2140.

Sikorski, R. J., & Zika, R. G. (1993). Modeling mixed-layer photochemistry of H_2O_2: Optical and chemical modeling of production. *Journal of Geophysical Research, 98*, 2315–2328.

Simpson, J. H., & Hunter, J. R. (1974). Fronts in the Irish Sea. *Nature, 250*, 404–406.

Smayda, T. J. (1970). The suspension and sinking of phytoplankton in the sea. *Oceanography and Marine Biology. An Annual Review, 8*, 353–414.

Smith, P. C. (1983). The mean and seasonal circulation off southwest Nova Scotia. *Journal of Physical Oceanography, 13*, 1034–1054.

Smith, P. C. (1989). Seasonal and interannual variability of current, temperature and salinity off southwest Nova Scotia. *Canadian Journal of Fisheries and Aquatic Sciences, 46*, 4–20.

Smith, R. C., & Baker, K. S. (1981). Optical properties of the clearest natural waters (200–800 nm). *Applied Optics, 20*, 177–184.

Sutcliffe, W. H., Jr., Loucks, R. H., & Drinkwater, K. F. (1976). Coastal circulation and physical oceanography of the Scotian Shelf and Gulf of Maine. *Journal of the Fisheries Research Board of Canada, 33*, 98–115.

Sverdrup, H. U. (1953). On conditions for the vernal blooming of phytoplankton. *J. Cons. Int. Explor. Mer., 18*, 287–295.

Townsend, D. W. (1989, March 6–7, 1989). The implications of slope water intrusions in the Gulf of Maine. Paper presented at the ARGO- Maine workshop.

Townsend, D. W. (1991). Influences of oceanographic processes on the biological productivity of the Gulf of Maine. *Reviews in Aquatic Sciences, 5*(3–4), 211–230.

Townsend, D. W. (1998). Sources and cycling of nitrogen in the Gulf of Maine. *Journal of Marine Systems, 16*, 283–295.

Townsend, D. W., Pettigrew, N. R., & Thomas, A. C. (2001). Offshore blooms of the red tide dinoflagellate, Alexandrium sp., in Gulf of Maine. *Continental Shelf Research, 21*(4), 347–369.

Troy, P. J., Li, Y.-H., & MacKenzie, F. T. (1997). Changes in surface morphology of calicite exposed to the oceanic water column. *Aquatic Geochemistry, 3*, 1–20.

Vaillancourt, R. D., Brown, C. W., Guillard, R. R. L., & Balch, W. M. (2004). Light backscattering by phytoplankton algae and a heterotrophic bacterium measured with a multi-wavelength, fixed-angle backscattering meter. *Journal of Plankton Research, 26*(2), 191–212.

Wells, M. L. (1998). Marine colloids: A neglected dimension. *Nature, 391*, 530–531.

Whitehead, R. F., de Mora, S., Demers, S., Gosselin, M., Monfort, P., & Mostajir, B. (2000). Interactions of ultraviolet-B radiation, mixing, and biological activity on photobleaching of natural chromophoric dissolved organic matter: A mesocosm study. *Limnology and Oceanography, 45*(2), 278–291.

Wong, C. S., Whitney, F. A., Crawford, D. W., Iseki, K., Matear, R. J., Johnson, W. K., Page, J. S., & Timothy, D. (1999). Seasonal and interannual variability in particle fluxes of carbon nitrogen and silicon from time series of sediment traps at Ocean Station P, 1982–1993: relationship to changes in subarctic primary productivity. *Deep-Sea Research II, 46*(11–12), 2735–2760.

Yentsch, C. S., & Garfield III, N. (1981). Principal areas of vertical mixing in the waters of the Gulf of Maine, with reference to the total productivity in the area. In J. F. R. Gower (Ed.), *Oceanography from space* (pp. 303–312). New York: Plenum.